

1 **Oxygenated VOCs as significant but varied contributors**
2 **to VOC emissions from vehicles**

3 Sihang Wang^{1,2}, Bin Yuan^{1,2,*}, Caihong Wu^{1,2}, Chaomin Wang^{1,2}, Tiange Li^{1,2}, Xianjun
4 He^{1,2}, Yibo Huangfu^{1,2}, Jipeng Qi^{1,2}, Xiao-Bing Li^{1,2}, Qing'e Sha^{1,2}, Manni Zhu^{1,2},
5 Shengrong Lou³, Hongli Wang³, Thomas Karl⁴, Martin Graus⁴, Zibing Yuan^{5*}, Min
6 Shao^{1,2}

7 ¹ Institute for Environmental and Climate Research, Jinan University, Guangzhou
8 511443, China

9 ² Guangdong-Hongkong-Macau Joint Laboratory of Collaborative Innovation for
10 Environmental Quality, Guangzhou 511443, China

11 ³ State Environmental Protection Key Laboratory of Formation and Prevention of
12 Urban Air Pollution Complex, Shanghai Academy of Environmental Sciences,
13 Shanghai 200233, China

14 ⁴ Department of Atmospheric and Cryospheric Sciences, University of Innsbruck,
15 Innsbruck, Austria

16 ⁵ College of Environment and Energy, South China University of Technology,
17 University Town, Guangzhou 510006, China

18
19
20 *Correspondence to: Bin Yuan (byuan@jnu.edu.cn) and Zibing Yuan
21 (zibing@scut.edu.cn)

23 **Abstract:**

24 Vehicular emission is an important source for volatile organic compounds (VOCs) in
25 urban and downwind regions. In this study, we conducted a chassis dynamometer study
26 to investigate VOC emissions from vehicles using gasoline, diesel, and liquefied
27 petroleum gas (LPG) as fuel. Time-resolved VOC emissions from vehicles are
28 chemically characterized by a proton-transfer-reaction time-of-flight mass
29 spectrometry (PTR-ToF-MS) with high frequency. Our results show that emission
30 factors of VOCs generally decrease with the improvement of emission standard for
31 gasoline vehicles, whereas variations of emission factors for diesel vehicles with
32 emission standards are more diverse. Mass spectra analysis of PTR-ToF-MS suggest
33 that cold start significantly influence VOCs emission of gasoline vehicles, while the
34 influences are less important for diesel vehicles. Large differences of VOC emissions
35 between gasoline and diesel vehicles are observed with emission factors of most VOC
36 species from diesel vehicles were higher than gasoline vehicles, especially for most
37 oxygenated volatile organic compounds (OVOCs) and heavier aromatics. These results
38 indicate quantification of heavier species by PTR-ToF-MS may be important in
39 characterization of vehicular exhausts. Our results suggest that VOC pairs (e.g. C₁₄
40 aromatics/toluene ratio) could potentially provide good indicators for distinguishing
41 emissions from gasoline and diesel vehicles. The fractions of OVOCs in total VOC
42 emissions are determined by combining measurements of hydrocarbons from canisters
43 and online observations of PTR-ToF-MS. We show that OVOCs contribute $9.4\% \pm 5.6\%$
44 of gasoline vehicles of the total VOC emissions, while the fractions are significantly
45 higher for diesel vehicles (52-71%), highlighting the importance to detect these OVOC
46 species in diesel emissions. Our study demonstrated that the large number of OVOC
47 species measured by PTR-ToF-MS are important in characterization of VOC emissions
48 from vehicles.

49

50 **1. Introduction**

51 Volatile organic compounds (VOCs) are important trace components in the
52 troposphere, as important precursors of ground-level ozone (Shao et al., 2009) and
53 secondary organic aerosol (SOA) (Seinfeld and Pandis, 2006;Kansal, 2009;Ziemann
54 and Atkinson, 2012). As the result, it is particularly important to identify emission
55 sources of VOCs in the atmosphere. Vehicular emission is an important source of VOCs
56 in cities around the world (Liu et al., 2008;Parrish et al., 2009), contributing
57 approximately 25% to total VOC emissions in China (Ou et al., 2015;Wu et al.,
58 2016;Sun et al., 2018). In order to control atmospheric pollution in urban and
59 surrounding regions, it is necessary to understand source profiles and emission
60 characteristics of VOCs from vehicles.

61 Emissions of VOCs from vehicles have been investigated extensively from
62 tunnel studies (Cui et al., 2018;Zhang et al., 2018;Song et al., 2020), on-road mobile
63 measurements (Li et al., 2017), and chassis dynamometer tests (Guo et al., 2011;Wang
64 et al., 2013;Yang et al., 2018). Previous studies demonstrated that fuel types of vehicles
65 strongly impact VOC emissions. Aromatics along with other hydrocarbons are known
66 as compounds with high emissions in exhausts of gasoline vehicles (Wang et al.,
67 2013;Ly et al., 2020). Some carbonyl compounds contribute significantly to emissions
68 of diesel vehicles, at fractions much higher than gasoline vehicles (Tsai et al., 2012;Qiao
69 et al., 2012;Yao et al., 2015;Mo et al., 2016). Moreover, there are still a large number
70 of unidentifiable compounds in diesel vehicles (May et al., 2014). Furthermore, VOC
71 emissions from vehicles significantly decreased in China due to stricter emission
72 standards (Liu et al., 2017;Sha et al., 2021). In order to reduce emissions of most
73 primary pollutants, more stringent emission standards and after-treatment devices have
74 been implemented. The emission standard of China VI has already been implemented
75 in July of 2019 in a few key cities in China and in July of 2021 nationwide. The emission
76 limits for various air pollutants emitted by vehicles are significantly lower under the
77 China VI emission standard (see details in the Supplement) (Wu et al., 2017). With the
78 continuous development of engine and exhaust after-treatment technologies, emission

79 characteristics of VOCs from vehicles may change and need to be frequently updated.

80 Oxygenated volatile organic compounds (OVOCs) were found to be an important
81 class of compounds in vehicle exhausts, accounting for more than 50% of the total VOC
82 emissions for diesel vehicles from both chassis dynamometer tests (Schauer et al.,
83 1999; Mo et al., 2016) and on-road mobile measurements (Yao et al., 2015).
84 Traditionally, VOCs are collected in the canister or Tedlar bags, and then analyzed by
85 gas chromatography-mass spectrometer/flame ionization detector (GC-MS/FID),
86 mainly reporting emissions of hydrocarbons (Wang et al., 2017; Qi et al., 2019).
87 Previous work usually collected 2,4-dinitrophenylhydrazine (DNPH) cartridges and
88 analyzed using high-performance liquid chromatography (HPLC) for carbonyls
89 (aldehydes and ketones), which are both time-consuming and prone to contaminations
90 (Mo et al., 2016; Han et al., 2019).

91 The large variability of VOC emissions under different engine activities or
92 driving conditions require characterization of vehicular emissions at higher time
93 resolution. Proton-transfer-reaction mass spectrometry (PTR-MS) has been used in a
94 number of studies for measurements of vehicle emissions. VOCs from vehicle exhausts
95 under various driving and operational modes were measured by PTR-MS onboard a
96 mobile laboratory (Zavala et al., 2006; Zavala et al., 2009). Drozd et al. (2016) used a
97 PTR-MS to emphasize the importance of cold start for vehicles, concluding that VOC
98 emissions during cold start were equal to a 200 miles distance of driving during hot
99 stabilized condition. Proton-transfer-reaction time-of-flight mass spectrometry (PTR-
100 ToF-MS) can provide more powerful detection of various VOCs, thanks to the
101 measurements of whole mass spectra and high mass resolution (Cappellin et al.,
102 2012; Yuan et al., 2017). More OVOC species could be quantified from the measured
103 mass spectra based on parameterization methods for sensitivity of instrument
104 (Sekimoto et al., 2017; Wu et al., 2020).

105 In this study, we applied a PTR-ToF-MS along with a suite of other instruments
106 to measure VOCs emitted from gasoline, diesel, and liquefied petroleum gas (LPG)
107 vehicles. We investigated emission factors from different fuel types and emission
108 standards for representative VOC species exhausted from these vehicles. We used the

109 dataset to analyze contributions of various VOC groups to total VOC emissions in
110 different types of vehicles.

111 **2. Materials and methods**

112 **2.1 Tested vehicles and the chassis dynamometer study methods**

113 In this study, we conducted chassis dynamometer measurements to investigate
114 VOC emissions from vehicles using gasoline, diesel, LPG as fuel. All gasoline vehicles
115 are light-duty-gasoline-vehicle (LDGV) with the emission standards from China I to
116 China VI, whereas diesel vehicles can be classified into light-duty-diesel-truck (LDDT),
117 middle-duty-diesel-truck (MDDT), heavy-duty-diesel-truck (HDDT), and bus
118 associated with emission standards of China III to China V. In addition, the test vehicles
119 using LPG are all taxis, which are under mandatory scrappage after 8 years of driving
120 in China; as a result only China IV and China V for LPG vehicles were tested. After-
121 treatment devices commonly used in light-duty gasoline vehicles are three-way catalyst
122 (TWC) and gasoline particulate filter (GPF) (Lyu et al., 2020). They have been
123 improved with the stricter emission standards. For diesel vehicles, typical after-
124 treatment devices include diesel oxidation catalyst (DOC), diesel particulate filter
125 (DPF), and selective catalyst reduction (SCR) (Zhou et al., 2019;Lyu et al., 2020;Shen
126 et al., 2021). The diesel vehicles for China III or prior do not have any after-treatment
127 devices. Light-duty-diesel-truck (LDDT) used DOC and DOC+DPF as after-treatment
128 devices in China IV and V diesel vehicles, respectively. SCR devices are mainly used
129 for heavy-duty-diesel-truck (HDDT) with China IV and V as after-treatment devices.
130 The fractions of gasoline and diesel vehicles with different emission standards in China
131 are shown in Table S1 (MEEPRC, 2019;Li et al., 2021). Among the 38 vehicles we
132 tested, a fraction of vehicles was measured several times, with a total of 62 experiments
133 measured. The detailed information for test vehicles is summarized in Sect. 1 in the
134 Supplement, Table S2 and Table S3.

135 The short transient driving cycle (GB 18285-2018, Figure S1a), as one of the
136 widely used test methods for vehicle emissions in China (Li et al., 2012;Wang et al.,
137 2013), was used for measurements of gasoline vehicles and LDDT, each running for

138 three to five times. The short transient driving cycle methods were initially adapted
139 based on emission regulations of the Economic Commission for Europe (ECE) cycle
140 (Yao et al., 2003), which is developed and used in European countries (Laurikko, 1995).
141 The short transient driving cycle consist of four conditions, namely idling, acceleration,
142 deceleration and uniform speed, as shown in Fig. S1. For the MDDT and HDDT, we
143 customized a step-by-step test method, in which the vehicle accelerates to 20 km·h⁻¹,
144 40 km·h⁻¹ and 60 km·h⁻¹ in sequence after the engine activates, keeping at 20 km·h⁻¹
145 and 40 km·h⁻¹ for 2 minutes, and 60 km·h⁻¹ for 1 minute, respectively (Fig. S1) (Li et
146 al., 2021;Liu et al., 2021;Liao et al., 2021). In addition, the cold start was tested for a
147 number of vehicles after a cold soak for more than 12 hours at ambient temperature
148 (20-25 °C) before engine started. The measurements of cold start are compared to
149 measurements of hot start after a ~10 minutes break for the vehicles after previous
150 measurement. More details about cold start and hot start in this campaign can be found
151 in Li et al. (2021).

152 A custom-built sampling and dilution system for vehicles combining online and
153 offline sampling techniques was used in this study. As shown in Fig. S2, a portable
154 emission measurement system (PEMS, SEMTECH-DS, Sensors. USA) was employed
155 to measure emissions of CO, CO₂, NO_x, and total hydrocarbon (THC) directly from the
156 tailpipe of vehicles. A custom-built dilution system (Li et al., 2021;Liao et al., 2021)
157 was used for dilution of vehicular emissions, achieving dilution ratios of 10-100 for
158 different vehicles. After dilution, CO₂ and CO were measured using a Li-840A
159 CO₂/H₂O Gas Analyzer (Licor, Inc. USA) and a Thermo 48i-TLE analyzer (Thermo
160 Fisher Scientific Inc. USA), respectively. Measurements of CO₂ before and after the
161 dilution system was used to determine the dilution ratio for each test (see details in Fig.
162 S3).

163 **2.2 VOC measurements using PTR-ToF-MS**

164 In this study, a Proton Transfer Reaction Quadrupole interface Time-of-Flight
165 Mass Spectrometer (PTR-QiToF-MS) (Ionicon Analytik, Innsbruck, Austria) with
166 H₃O⁺ chemistry was used to measure VOCs (Sulzer et al., 2014). The mass spectra of

167 PTR-ToF-MS was recorded every 1 s as to capture characteristics of VOC species from
168 vehicle exhausts in real-time. Background measurements of the instrument were
169 performed using sampled air through a custom-built platinum catalytical converter
170 heated to 365 °C for 30 s before vehicle starts in each test. The more detailed setting
171 parameters for the instrument can be found elsewhere (Wu et al., 2020;Wang et al.,
172 2020a;He et al., 2022). Data analysis of PTR-ToF-MS was performed using the Tofware
173 software package (version 3.0.3, Tofwerk AG, Switzerland) (Stark et al., 2015).

174 A 23-component gas standard (Linde Spectra) was used for daily calibration of
175 PTR-ToF-MS during the campaign. VOC sensitivities from automatical calibrations
176 indicated quite stable instrumental performance for most of the VOC species (Fig. S4).
177 Another gas standard with 35-component VOCs (Apel Riemer Environmental Inc.) was
178 used for calibrations during the later period of this campaign to include more VOC
179 species in the calibration. The Liquid Calibration Unit (LCU, Ionicon Analytik,
180 Innsbruck, Austria) was used to calibrate a total of 11 organic acids and nitrogen-
181 containing species (Table S4). The limits of detection for calibrated VOC species are
182 below 100 ppt for the 1-s measurement, except for ethanol (423 ppt) and formic acid
183 (166 ppt). Additionally, the humidity dependence for a few VOC species in PTR-ToF-
184 MS (Yuan et al., 2017;Koss et al., 2018) were corrected using humidity-dependence
185 curves determined in the laboratory, as previously shown in Wu et al. (2020). To
186 quantify the ion signals without calibration, we determine the sensitivities based on the
187 kinetics of proton-transfer reactions of H_3O^+ with VOCs (Cappellin et al.,
188 2012;Sekimoto et al., 2017). The relationship between VOCs sensitivity and kinetic
189 rate constants for the same instrument has been reported in Wu et al. (2020) and He et
190 al. (2022). The corrected sensitivities as a function of kinetic rate constants for proton-
191 transfer reactions of H_3O^+ with VOCs during this campaign is shown in Fig. S5. The
192 fitted line is used to determine sensitivities of uncalibrated species, and the uncertainty
193 of the concentrations for uncalibrated species are determined to be around 50%.

194 **2.3 Other VOC measurements**

195 Whole air samples were collected using canisters after the dilution system for

196 determination of hydrocarbons emitted from various vehicles. All the canisters were
197 sent to the laboratory for analysis by an offline GC-MS/FID system, with a total 95
198 hydrocarbons calibrated by Photochemical Assessment Monitoring Stations (PAMS)
199 and TO-15 standard mixtures (Table S5). We compared emission factors from PTR-
200 ToF-MS and the offline canister-GC-MS/FID (Fig. S6c-d), obtaining generally
201 consistent results, considering the large variation of VOC emissions for driving
202 conditions and the difficulty to control the fill time for canisters.

203 An instrument based on Hantzsch reaction-absorption method was used to
204 measure formaldehyde (Zhu et al., 2020). Good agreement for formaldehyde between
205 PTR-ToF-MS and the Hantzsch instrument was obtained (Fig. S6a). An iodide-adduct
206 time-of-flight chemical ionization mass spectrometer (I⁻ ToF-CIMS, Aerodyne
207 Research, Inc.) (Wang et al., 2020c; Ye et al., 2021) was used to measure organic acids,
208 hydrogen cyanide (HCN), and isocyanic acid (HNCO) from vehicles (Li et al., 2021).
209 As shown in Fig. S6b, formic acid measured by PTR-ToF-MS and I⁻ ToF-CIMS showed
210 reasonable agreement.

211 **2.4 Emission factors and emission ratios calculation**

212 In this study, we determine emission factors of VOC species in two different
213 approaches: the mileage-based emission factors ($\text{mg}\cdot\text{km}^{-1}$) as the mass of these VOCs
214 exhausted per kilometer driving of vehicles, and the fuel-based emission factors
215 ($\text{mg}\cdot\text{kg}_{\text{fuel}}^{-1}$) as the mass of VOCs per kilogram of fuel burned by the vehicles. In
216 addition, emission ratios of VOCs to combustion tracers (usually CO) are widely
217 applied in vehicle emissions in urban regions, as the result we determine emission
218 ratios to CO in $\text{ppb}\cdot\text{ppm}^{-1}$ as well. More details about the determination of emission
219 factors and emission ratios can be found in Sect. 2 in the Supplement.

220 The average emission factors for various types of vehicles are determined from
221 arithmetic means for different emission standards of vehicles. As for diesel vehicles,
222 the average emission factors are obtained from the arithmetic means of LDDT, MDDT,
223 HDDT, and bus. Besides, we also calculate emission factors and emission ratios from
224 weighted means based on the fractions of gasoline and diesel vehicles with different

225 emission standards in China (MEEPRC, 2019;Li et al., 2021) (see Sect. 2 in the
226 Supplement for details). In order to evaluate the uncertainties of obtained emission
227 factors, the average limit of detection for VOC species are used to estimate the limit
228 of detection for the determined emission factors (more details can be found in Sect. 3
229 in the Supplement).

230 **3. Results and discussions**

231 **3.1 Characteristics of the VOC emissions in the vehicles**

232 Time series of several aromatics and OVOC species measured by PTR-ToF-MS
233 for a selected gasoline vehicle associated with emission standard of China I and a LDDT
234 associated with China IV emission standard are shown in Fig. 1. Both tests started with
235 cold engines for the two vehicles. Benzene and toluene are typical aromatic species
236 emitted by vehicles. As shown in Fig. 1a, high concentrations of benzene and toluene
237 exhausted by the gasoline vehicle were observed as the engine started. The
238 concentrations of the two species continued to increase until ~2 min after the engine
239 started, and then dropped rapidly before a minor increase during the acceleration
240 condition. These observations are similar to the previous results from PTR-MS
241 measurements in Drozd et al. (2016). Acetaldehyde and acetone are important OVOC
242 species emitted from vehicles. They show similar temporal variations as benzene and
243 toluene. However, concentrations of acetaldehyde and acetone were much lower than
244 the two aromatics after engine started. Compared to the concentrations at engine start-
245 up for the gasoline vehicle (the first cycle), concentrations of the VOCs are 3.0 to 40
246 times lower during the gasoline vehicle running at hot stabilized condition (the third
247 cycle). As shown in Fig. 1 for the diesel vehicle, enhanced emissions from cold start
248 are minor, which is different from the gasoline vehicle. The concentration of these
249 VOCs at engine start-up for the diesel vehicle are only 1.3 to 2.5 times higher than the
250 periods as the diesel vehicle running at hot stabilized condition. It indicates that the
251 impact of the engine start-up in diesel vehicles on emissions is much lower than
252 gasoline vehicles. It might be a combined effect of cold engine and operation
253 temperature of the after-treatment device (Gentner et al., 2017;George et al., 2015). In

254 contrast to the gasoline vehicle, we observe higher concentrations of the two OVOC
255 species than the two aromatics species from the diesel vehicle. These higher OVOC
256 concentrations in diesel vehicle exhausts are in line with the observations of organic
257 acids using the I-ToF-CIMS from the same campaign (Li et al., 2021).

258 Based on the high time-resolution measurements of PTR-ToF-MS, we
259 determined emission factors of various VOC species from different vehicles. Fig. 2
260 shows the determined average mileage-based emission factors of benzene, toluene,
261 acetaldehyde, and acetone for various types of vehicles (also tabulated in the
262 Supplement table). In general, we observe a downward trend for emissions factors of
263 gasoline vehicles from China I to China VI emission standards for the four
264 representative VOC species. This is consistent with the results in previous studies with
265 lower emissions for newer emission standards (Wang et al., 2017; Sha et al., 2021). In
266 addition, the dependence of VOCs emission versus emission standard may also be
267 attributed to the history of vehicle usage, i.e., the mileage traveled by the vehicles, as
268 lower mileages of vehicles are usually associated with vehicle with newer emission
269 standards. As shown in Fig. 3, we observe strong positive relationship between toluene
270 emission factors and vehicle odometers for both gasoline and diesel vehicles, indicating
271 the mileages of vehicles can significantly affect VOCs emission factors for vehicles
272 tested in this study. The emission factors of the representative VOC species are highest
273 for China II gasoline vehicles rather than China I vehicles, which can be explained by
274 the China II vehicles having the highest mileage of the test vehicles.~~Intestinally, the~~
275 ~~emission factors of the representative VOC species are highest for China II gasoline~~
276 ~~vehicles rather than China I vehicles, coincidence with largest mileage of the test~~
277 ~~vehicles.~~ Emission factors of the four species for China VI vehicles are 12 to 25 times
278 lower than emissions for China I vehicles, indicating that newer emission standards
279 successfully reduced VOC emissions of gasoline vehicles. The decline of emission
280 factors for the four species with newer emission standards for diesel vehicles are in the
281 range of 1.1 to 7.4 times from China III to China V, compared to 4.5 to 5.4 times
282 reduction from China III to China V for gasoline vehicles. Emission factors of benzene
283 and toluene from diesel vehicles are in the range of 0.8 to 7.4 mg·km⁻¹ and 0.3 to 5.8

284 $\text{mg}\cdot\text{km}^{-1}$, which are comparable to emission factors from gasoline vehicles with China
285 IV to China VI emission standards. This is different from observations of the two
286 OVOC species (acetaldehyde and acetone), with much higher emission factors from
287 diesel vehicles (8.0 to $27.9 \text{ mg}\cdot\text{km}^{-1}$ for acetaldehyde and 0.8 to $10.0 \text{ mg}\cdot\text{km}^{-1}$ for
288 acetone) than almost all gasoline vehicles (a maximum of $3.9 \text{ mg}\cdot\text{km}^{-1}$ for acetaldehyde
289 and a maximum of $3.2 \text{ mg}\cdot\text{km}^{-1}$ for acetone). Higher emission factors from diesel
290 vehicles are also observed for many other common OVOC species, as shown in Fig. 4.
291 As the largest OVOCs emitted from gasoline vehicles ($4.6 \pm 5.1 \text{ mg}\cdot\text{km}^{-1}$), methanol is
292 found to be the only common OVOC species, with lower emission factors from diesel
293 vehicles than gasoline vehicles. The emission factor of other OVOCs (e.g.
294 formaldehyde, acetone) from diesel vehicles are higher than gasoline vehicles, which
295 is consistent with previous results (Gentner et al., 2013). The high emissions of OVOCs
296 from diesel vehicles may be related to combustion processes in diesel vehicles, with
297 more excess air (i.e., under overall fuel-lean conditions) into combustion cylinder
298 resulting in higher oxygen contents and more oxidation processes during fuel
299 combustion (Pang et al., 2008; Qiao et al., 2012; Gentner et al., 2017). Finally, the
300 determined emission factors of the four VOC species from LPG vehicles are much
301 lower than both gasoline and diesel vehicles.

302 **3.2 Analysis of PTR-ToF-MS mass spectra to evaluate VOCs** 303 **speciation**

304 In addition to typical VOC species shown above, PTR-ToF-MS detected
305 abundant signals for a large number of ions. The determined average mileage-based
306 emission factors for all detected VOC species are shown as mass spectra in Fig. 4. VOC
307 species measured by PTR-ToF-MS were divided into groups according to chemical
308 formula, namely hydrocarbon species only containing C and H atoms (C_xH_y), OVOCs
309 ($\text{C}_x\text{H}_y\text{O}_z$), species containing nitrogen and/or sulfur atoms (N/S-containing), and some
310 other ions (others). We observe similar mass spectra of emission factors for gasoline
311 vehicles with different emission standards (Fig. S7). Highest emission factors from
312 gasoline vehicles (Fig. 5a) are detected as hydrocarbons, including C_6 to C_{10} aromatics.

313 A few OVOC species, namely methanol, ethanol, formaldehyde, acetaldehyde and
314 acetone, are also observed as the largest emissions. In contrast to gasoline vehicles, the
315 largest emissions from diesel vehicles were attributed to a few low-molecular-weight
316 OVOC species, including formaldehyde, acetaldehyde, formic acid, and acetic acid,
317 followed by a large number of hydrocarbon species. Comparison between the mass
318 spectra of gasoline and diesel vehicle emissions suggest that emissions from diesel
319 vehicles are more evenly distributed among different VOC species, as reflected by 50
320 and 140 species contributing more than 1% of the total emissions for gasoline and diesel
321 vehicles, respectively. As shown in Fig. 5b, many hydrocarbon ions in the range of m/z
322 150-200 still account for significant fractions of emissions from diesel vehicles,
323 whereas only one species in this m/z range contribute more than 1% of emissions from
324 gasoline vehicles. These results demonstrate that diesel vehicles emit more heavier
325 hydrocarbons than those from gasoline vehicles, which is consistent with observations
326 in previous studies (Gentner et al., 2012; Erickson et al., 2014). ~~It should be noted that
327 the signals of $C_{16}H_{22}O_4H$ ($m/z=279$) were higher during the tests based on determined
328 emission factors. However, we suspect that it may be emitted artifacts from the
329 sampling or dilution system as it mainly showed higher signals in the latter period of
330 each test when sampling materials absorb more heat from vehicle exhausts (Fig. S8),
331 and thus it is not included in Fig. 5 (details in the Sect. 3 in the Supplement).~~

332 The scatterplot of carbon oxidation states (\overline{OS}_C) as a function of carbon number
333 (n_C) provides a framework for describing bulk chemical properties of organics (Kroll
334 et al., 2011). The details of \overline{OS}_C calculation is included in Sect. 4 in the Supplement.
335 The results from gasoline and diesel vehicles are compared in Fig. 6 (LPG vehicles are
336 shown in Fig. S89). It is apparent that ions with carbon oxidation states between -2.0 to
337 0 comprise main emissions for each carbon number for both gasoline and diesel
338 vehicles. It is interesting to observe that averaged \overline{OS}_C for $n_C > 6$ increase as the carbon
339 number decrease for both gasoline and diesel vehicles, whereas the opposite trends are
340 observed for $n_C < 5$. The averaged \overline{OS}_C in diesel vehicles for n_C between 1 and 5 are
341 significantly higher than those in gasoline vehicles, as the result of high emissions of
342 C_2 to C_5 low-molecular-weight OVOCs. Fig. 6c further shows that emission factors of

343 most VOC species from diesel vehicles were higher than gasoline vehicles, except a
344 number of species occupying in the right-bottom corner of the two-dimensional space.

345 The determined mass spectra of PTR-ToF-MS in terms of emission factor for
346 different types of vehicles can be used to explore the dependence of various VOC
347 emissions to different factors. Fig. 7a-b shows scatterplots of the average mileage-
348 based emission factors of VOCs between cold start and hot start for gasoline and diesel
349 vehicles, respectively. We observe strong correlation between emission factors from
350 cold start and hot start tests ($R=0.99$ and 0.92) and generally consistent ratios between
351 cold start and hot start for different types of VOC species for both gasoline and diesel
352 vehicles, indicating that variation behaviors are similar for different species and thus
353 chemical compositions of VOC emissions are comparable between different start
354 conditions. As cold start emissions are richer in unburned fuel than other hot-running
355 conditions (Gentner et al., 2017) and the after-treatment devices aim for VOCs control
356 for gasoline vehicles, the strong correlation and significantly lower slope than unity in
357 Fig. 7a, ~~the observation in Fig. 7a-b also~~ infer that unburned fuel are the major
358 contributor for ~~vehicle~~ exhaust emissions of gasoline vehicles, which has been
359 previously shown in California, U.S. (Gentner et al., 2013). It is obvious that emission
360 factors of VOCs during cold start are significantly higher than those during hot start
361 for gasoline vehicles (slope= 0.40), whereas similar emissions factors between cold
362 start and hot start are derived for diesel vehicles (slope= 0.84). These results suggest
363 that gasoline vehicles are more significantly influenced by cold start, as the result of
364 compositions in gasoline fuel are more volatile than diesel fuel (US NRC, 1996). We
365 further explore the effects of emission standards to VOCs emission factors by
366 comparing determined emission factors between China I and China V for gasoline
367 vehicle (Fig. 7c, also see China III versus China V and China V versus China VI in
368 Fig. S910) and between China III and China V for LDDT (Fig. 7d, also see China III
369 versus China V for MDDT and HDDT in Fig. S910). Fig. 7c-d show that the chemical
370 compositions of VOC emissions are comparable between different emission standards
371 for abundant VOC species from gasoline vehicles, both gasoline and diesel vehicles
372 ($R=0.98$ and 0.89), indicating after-treatment devices may not affect the relative

373 fractions of VOC components for gasoline vehicles (Drozd et al., 2019;Lu et al.,
374 2018;Zhao et al., 2017). In comparison, the results between different emission
375 standards for diesel vehicles (Fig. 7d) are somewhat larger than in gasoline vehicles.
376 Furthermore, comparison of both gasoline and diesel vehicles demonstrate newer
377 emission standards successfully decreased VOC emissions. Based on the derived
378 slopes, we obtain VOCs emission factors reduced by a factor of 10 for gasoline
379 vehicles from China I to China V (a factor of 5 reduction from China III to China V
380 and a factor of 2.5 reduction for China V to China VI), and a factor of 2 reduction for
381 LDDT from China III to China V (a factor of 1.5 and 8 reduction for MDDT and
382 HDDT from China III to China V). The reduction ratio for gasoline vehicles from
383 China I to China V are generally similar for most VOC species, except that some
384 OVOC species with smaller reduction ratios. The reduction ratios for LDDT vehicles
385 from China III to China V show large variability for different species. The lowest
386 reduction ratios (a factor of ~2) are observed for the low-molecular weight OVOC
387 species associated with largest emissions, while the reduction ratios for hydrocarbons
388 and higher-molecular weight OVOCs are in the range of a factor of 10-100. These
389 results indicate the after-treatment device for diesel vehicles (see Sect. 1 in the
390 Supplement for details.) may effectively reduce emissions of some heavier VOC
391 species, though the after-treatment devices do not aim for VOCs control (Gentner et
392 al., 2017).

393 **3.3 Non-target analysis for comparison between gasoline and diesel** 394 **vehicles**

395 As shown in the previous section, the analysis of PTR-ToF-MS mass spectra
396 provide rich information on understanding the influences of VOC emissions from
397 vehicles. This detailed information provided by the PTR-ToF-MS also offer an
398 opportunity to systematically compare emissions between gasoline and diesel vehicles.
399 The scatterplot of the determined average emission factors of various VOC species
400 between gasoline and diesel vehicles is shown in Fig. 8. Large difference of VOC
401 compositions emitted from gasoline and diesel vehicles are observed, as indicated by

402 the low correlation of the data points ($R=0.24$). A limited number of VOC species,
403 including C_6 - C_{10} aromatics and some N/S-containing species (e.g. C_7H_5N) are
404 associated with higher emission factors from gasoline vehicles, whereas the obtained
405 emission factors of most VOC species emitted from diesel vehicles are higher,
406 especially most OVOC species. For example, formic acid is found to be one of the
407 most significant emission species in diesel vehicles, with emission factors three orders
408 of magnitude higher than that of gasoline vehicles. In addition, emission factors of
409 HCN from gasoline vehicles are similar to those from diesel vehicles. These results
410 are consistent with the measurements using the I ToF-CIMS from the same campaign,
411 as shown in Li et al. (2021).

412 The scatterplot shown in Fig. 8 can also be expressed in terms of the determined
413 fuel-based emission factors between gasoline and diesel vehicles (Fig. S104a).
414 Generally, similar variability is obtained except the determined slope of the data points,
415 with higher slopes determined from the scatterplot based on fuel-based emission factor
416 (0.19 versus 0.15). The emission ratios to CO between gasoline and diesel vehicles
417 (Fig. S104b) show similar results. Furthermore, the difference between the slopes
418 reflects the different average mileage for the same weight of fuel between gasoline
419 ($9.7 \text{ km}\cdot\text{kg}_{\text{fuel}}^{-1}$) and diesel vehicles ($7.1 \text{ km}\cdot\text{kg}_{\text{fuel}}^{-1}$), as demonstrated for emission
420 factors of CO_2 in Table S6.

421 Comparing gasoline and diesel vehicles, we can also observe profound
422 differences in relative changes of emission factors for analogous compounds series. The
423 emission factors of C_6 - C_{10} aromatics are apparently higher for gasoline vehicles than
424 diesel vehicles, whereas emission factors for larger aromatics ($n_c > 11$) from diesel
425 vehicles start to exceed gasoline vehicles. This interesting behavior is the result of
426 different variations of emission factors for gasoline and diesel vehicles as carbon
427 number increases. This may be attributed to the differences of chemical compositions
428 of gasoline and diesel fuel, such as higher fractions of polycyclic aromatic
429 hydrocarbons (PAHs) in the diesel fuel (Yue et al., 2015; Gentner et al., 2017). As shown
430 in Fig. 9, emission factors of aromatics from gasoline vehicles start to rapidly decrease
431 at $n_c=10$ (a factor of 5 for each additional carbon for C_{10} - C_{15}), while the emission

432 factors of aromatic for diesel vehicles demonstrate a relatively flat pattern between C₆
433 and C₁₅, only with significantly decrease for $n_c > 15$. Based on Fig. 9, we determine that
434 emissions of aromatics with $n_c \geq 10$ in gasoline and diesel vehicles are account for 14%
435 and 63% of total aromatic emissions, again suggest the importance of heavier aromatics
436 in emissions from diesel vehicles. It also highlights that quantification of these heavier
437 species by PTR-ToF-MS may be important in characterization of vehicular exhausts,
438 especially diesel vehicles.

439 In addition to aromatics, the relative changes of emission factors for carbonyls
440 with carbon number are apparently different between gasoline and diesel vehicles (Fig.
441 8 and Fig. 9b). Emission factors of carbonyls tend to decrease as carbon number
442 increase for both gasoline and diesel vehicles. The decrease magnitudes are observed
443 to be comparable from C₁-C₆ carbonyls for gasoline (97.6%) and diesel vehicles
444 (97.4%). However, as $n_c > 6$, the decrease of carbonyl emissions factors for diesel
445 vehicles become smaller, result in larger emissions factors than gasoline vehicles for
446 this range of carbon number.

447 The above discussions demonstrate that emission characteristics of aromatics and
448 OVOCs are significantly different between gasoline and diesel vehicles. As the result,
449 the ratios of VOC pairs can be identified to distinguish emissions of gasoline and diesel
450 vehicles. Fig. 10 shows the scatterplots of four representative VOCs (benzene, C₁₄
451 aromatics, formaldehyde, and acetaldehyde) versus toluene based on the determined
452 emission factors. The data points for each VOCs pair clearly show distinct separation
453 between gasoline vehicles and diesel vehicles, with apparently higher slopes for diesel
454 vehicles than gasoline vehicles, as the result of much larger emission factors of toluene
455 from gasoline vehicles and lower emission factors of the four representative VOCs
456 from diesel vehicles. The benzene/toluene ratio in gasoline and diesel vehicle are
457 determined as 0.48 and 1.24 mg·mg⁻¹ (corresponding to 0.57 and 1.46 ppb·ppb⁻¹ that
458 are more widely used in ambient studies). The difference of benzene/toluene ratio
459 between gasoline and diesel vehicles has been reported in previous studies, and our
460 results are generally consistent with these previous results (Chan et al., 2002; Barletta
461 et al., 2005; Qiao et al., 2012; Kumar et al., 2020). Compared to benzene/toluene ratio,

462 the difference of C₁₄ aromatics/toluene ratio between gasoline and diesel vehicles are
463 more substantial (a factor of 3800). The significantly higher emission factors of C₁₄
464 aromatics from diesel vehicles suggest that diesel vehicles can be a significant or even
465 dominant source for higher molecular-weight aromatics.~~The remarkable larger~~
466 ~~emission factors of C₁₄ aromatics from diesel vehicles suggest that diesel vehicles can~~
467 ~~be a significant or even predominated source for higher molecular aromatics.~~ The
468 enormous difference of C₁₄ aromatics/toluene ratio (and also other higher
469 aromatics/toluene) between gasoline and diesel vehicles indicate these ratios could
470 potentially provide good indicators for separation of gasoline and diesel vehicles in
471 ambient or tunnel studies (see discussion in Sect. 5 in the Supplement for details about
472 the feasibility of the ratio using in ambient air). Similar discrepancies are observed for
473 formaldehyde/toluene and acetaldehyde/toluene ratios between gasoline and diesel
474 vehicles. These ratios may not be able to be used as indicators for distinguish gasoline
475 and diesel vehicles in ambient studies, since secondary sources may complicate the
476 observed ratios in ambient air. However, these results strongly suggest that diesel
477 vehicles can be important in emissions of these OVOC species, though the number of
478 diesel vehicles are smaller than gasoline vehicles in many countries, e.g. China and
479 U.S (Wallington et al., 2013; Yao et al., 2015; Huang et al., 2021).

480 **3.4 OVOC fractions in VOC emissions**

481 Emission factors of various VOC species measured by PTR-ToF-MS from
482 different vehicles are summarized in Fig. 11. As shown in Fig. 11a, the determined
483 average mileage-based emission factors of total VOC ions from diesel vehicles were
484 much higher than gasoline and LPG vehicles. Fig. 11b-d quantified the proportions of
485 different categories of ions measured by PTR-ToF-MS. The determined average
486 mileage-based emission factors of C_xH_y accounted for the largest fraction in gasoline
487 vehicles (84% ± 5.9%), and lower fractions in diesel (47% ± 16%) and LPG vehicles
488 (32% ± 0.7%). OVOCs account for larger fractions in diesel (49% ± 16%) and LPG
489 vehicles (58% ± 3.7%), while they only account for 13% ± 6.1% of emissions from
490 gasoline vehicles. The fractions of different OVOC groups generally demonstrate a

491 downward trend from $C_xH_yO_1$ to $C_xH_yO_{\geq 3}$, and OVOCs with more than two oxygen
492 atoms only occupy small percentages (0-7%) in vehicle exhausts, indicating low
493 emissions of these species.

494 Combined with measurements of other VOCs from canisters measured by GC-
495 MS/FID, the fractions of OVOCs in total VOC emissions can be determined for
496 different vehicles (details in Sect. 6 in the Supplement) (Fig. 12). OVOCs account for
497 $9.4\% \pm 5.6\%$ of total VOC emissions for gasoline vehicles. The OVOC fractions for
498 gasoline vehicles are generally comparable for different emission standards and
499 cold/hot start, except somewhat higher fractions for China VI from hot start (Fig. S112).
500 The OVOC fractions obtained in this study for gasoline vehicles are generally
501 consistent with previous results (Cao et al., 2016; Wang et al., 2020b) (Fig. 12). Among
502 these studies, the OVOC fractions determined for gasoline with 10% ethanol (E10)
503 (Roy et al., 2016) ($22\% \pm 11\%$) are apparently higher. The fractions of OVOCs in total
504 VOC emissions for diesel vehicles are $71\% \pm 20\%$, $65\% \pm 22\%$, $52\% \pm 18\%$, and 56%
505 $\pm 26\%$ for LDDT, MDDT, HDDT, and bus, respectively. The variations of OVOC
506 fractions with emission standards are observed to be mixed among different types of
507 diesel vehicles (Fig. S112). The OVOC fractions from diesel vehicles are obviously
508 higher than those in gasoline vehicles, indicating the importance of OVOCs in VOC
509 emissions for diesel vehicles. Compared to previous studies (Tsai et al., 2012; Qiao et
510 al., 2012; Cao et al., 2016; Mo et al., 2016), determined OVOC fractions for diesel
511 vehicles in this study are higher. If only considering carbonyls among various types of
512 OVOCs measured by PTR-ToF-MS, the OVOC fractions determined in this study are
513 more comparable with previous studies (Fig. 12), since most previous studies only
514 detected carbonyls among various types of OVOCs. Finally, we determine that OVOCs
515 account for $41\% \pm 10\%$ of total VOC emissions for LPG vehicles, which is also higher
516 than in one previous study (Wang et al., 2020b) with only carbonyls and a few
517 esters/alcohols included. These results stress that the large number of OVOCs measured
518 by PTR-ToF-MS are important in characterization of VOC emissions from vehicles. It
519 should be noted that the OVOC fractions obtained here only reflect exhaust emissions.
520 Evaporative emissions may be associated with different fractions of various VOC

521 groups, which may be more related to fuel compositions (Rubin et al., 2006;Huang et
522 al., 2021).

523 **4. Conclusions**

524 In this work, we conducted a chassis dynamometer study to measure VOC
525 emissions from gasoline, diesel, and LPG vehicles using PTR-ToF-MS along with other
526 offline and online measurement techniques. Using this dataset, we provide emission
527 factors of many VOCs from these three different types of vehicles associated with
528 various emission standards in China. Our results show that emission factors of VOCs
529 generally decrease with the increased stringency of emission standards for gasoline
530 vehicles, whereas variations of emission factors for diesel vehicles with emission
531 standards are more diverse. Mass spectra analysis of PTR-ToF-MS suggest that cold
532 start significantly influence VOCs emission of gasoline vehicles, while the influences
533 are smaller for diesel vehicles.

534 We observe large differences of VOC emissions between gasoline and diesel
535 vehicles based on PTR-ToF-MS measurements. Emission factors of most VOC species
536 from diesel vehicles were higher than gasoline vehicles, especially for most OVOCs
537 and heavier aromatics. The substantially larger emission factors of some OVOCs
538 emission factors for diesel vehicles indicate potentially dominant emissions of these
539 species from diesel vehicles among vehicular emissions. Our results suggest that VOC
540 pairs (e.g. C₁₄ aromatics/toluene ratio) could potentially provide good indicators for
541 distinguishing emissions between gasoline and diesel vehicles.

542 Based on measurements of PTR-ToF-MS, C_xH_y ions account for the largest
543 fraction in gasoline vehicles (84% ± 5.9%), whereas OVOC ions are the largest
544 contributor in the mass spectra of emissions from diesel (49% ± 16%) and LPG vehicles
545 (58% ± 3.7%). In the end, the fractions of OVOCs in total VOC emissions are
546 determined by combining hydrocarbons measurements from canister results and online
547 measurements of PTR-ToF-MS. We show that OVOCs contribute 9.4% ± 5.6% of
548 gasoline vehicles of the total VOC emissions, while the fractions are significantly
549 higher for diesel vehicles (52-71%), highlighting the importance to detect these OVOC

550 species in diesel emissions.

551 This study shows significant contributions of OVOCs in VOC emissions from
552 various vehicles, especially diesel vehicles. As a consequence, vehicular emissions may
553 account for considerable proportions for primary emissions of these OVOCs in urban
554 regions. Emissions of many OVOC species are currently not fully represented in
555 emission inventories of VOCs, which may in turn affect the prediction ability of air
556 quality models in urban regions. In this study, OVOC species are mainly quantified
557 from PTR-ToF-MS measurements by taking into account all signals in the mass spectra,
558 which stress that the large number of OVOC species measured by PTR-ToF-MS are
559 important in characterization of VOC emissions from vehicles.

560 **Data availability**

561 Data are available from the authors upon request.

562 **Author contribution**

563 BY designed the research. ZBY, BY, QES organized vehicle test measurements.
564 SHW, CHW, CMW, TGL, JPQ, QES, and MMZ contributed to data collection. SHW
565 performed the data analysis, with contributions from TGL, XJH, YBH, XBL, and QES.
566 SHW and BY prepared the manuscript with contributions from other authors. All the
567 authors reviewed the manuscript.

568 **Competing interests**

569 The authors declare that they have no known competing financial interests or
570 personal relationships that could have appeared to influence the work reported in this
571 paper.

572 **Acknowledgement**

573 This work was supported by the National Key R&D Plan of China (grant No.
574 2019YFE0106300, 2018YFC0213904), the National Natural Science Foundation of
575 China (grant No. 41877302, 42121004), Guangdong Natural Science Funds for
576 Distinguished Young Scholar (grant No. 2018B030306037), Guangdong Basic and
577 Applied Basic Research Fund Project (grant No. 2020A1515110085), and Guangdong

578 Innovative and Entrepreneurial Research Team Program (grant No. 2016ZT06N263).
579 This work was also supported by Special Fund Project for Science and Technology
580 Innovation Strategy of Guangdong Province (Grant No.2019B121205004). TK and
581 MG were supported by OEAD grant CN 05/2020. The authors would like to thank Prof.
582 Junyu Zheng for providing many resources during vehicle measurements and allowing
583 to use PEMS and formaldehyde data in this study.

584

585 **References**

- 586 Permissible Exposure Levels for Selected Military Fuel Vapors, The National
587 Academies Press, Washington, DC, 1996.
- 588 Barletta, B., Meinardi, S., Sherwood Rowland, F., Chan, C.-Y., Wang, X., Zou, S., Yin
589 Chan, L., and Blake, D. R.: Volatile organic compounds in 43 Chinese cities,
590 Atmospheric Environment, 39, 5979-5990, 10.1016/j.atmosenv.2005.06.029, 2005.
- 591 Cao, X., Yao, Z., Shen, X., Ye, Y., and Jiang, X.: On-road emission characteristics of
592 VOCs from light-duty gasoline vehicles in Beijing, China, Atmospheric Environment,
593 124, 146-155, 10.1016/j.atmosenv.2015.06.019, 2016.
- 594 Cappellin, L., Karl, T., Probst, M., Ismailova, O., Winkler, P. M., Soukoulis, C., Aprea,
595 E., Mark, T. D., Gasperi, F., and Biasioli, F.: On quantitative determination of volatile
596 organic compound concentrations using proton transfer reaction time-of-flight mass
597 spectrometry, Environmental Science & Technology, 46, 2283-2290,
598 10.1021/es203985t, 2012.
- 599 Chan, C. Y., Chan, L. Y., Wang, X. M., Liu, Y. M., Lee, S. C., Zou, S. C., Sheng, G. Y.,
600 and Fu, J. M.: Volatile organic compounds in roadside microenvironments of
601 metropolitan Hong Kong, Atmospheric Environment, 36, 2039-2047,
602 [https://doi.org/10.1016/S1352-2310\(02\)00097-3](https://doi.org/10.1016/S1352-2310(02)00097-3), 2002.
- 603 Cui, L., Wang, X. L., Ho, K. F., Gao, Y., Liu, C., Hang Ho, S. S., Li, H. W., Lee, S. C.,
604 Wang, X. M., Jiang, B. Q., Huang, Y., Chow, J. C., Watson, J. G., and Chen, L.-W.:
605 Decrease of VOC emissions from vehicular emissions in Hong Kong from 2003 to 2015:
606 Results from a tunnel study, Atmospheric Environment, 177, 64-74,
607 10.1016/j.atmosenv.2018.01.020, 2018.
- 608 Drozd, G. T., Zhao, Y., Saliba, G., Frodin, B., Maddox, C., Weber, R. J., Chang, M. O.,
609 Maldonado, H., Sardar, S., Robinson, A. L., and Goldstein, A. H.: Time Resolved
610 Measurements of Speciated Tailpipe Emissions from Motor Vehicles: Trends with
611 Emission Control Technology, Cold Start Effects, and Speciation, Environmental
612 Science & Technology, 50, 13592-13599, 10.1021/acs.est.6b04513, 2016.
- 613 Drozd, G. T., Zhao, Y., Saliba, G., Frodin, B., Maddox, C., Oliver Chang, M. C.,
614 Maldonado, H., Sardar, S., Weber, R. J., Robinson, A. L., and Goldstein, A. H.: Detailed
615 Speciation of Intermediate Volatility and Semivolatile Organic Compound Emissions
616 from Gasoline Vehicles: Effects of Cold-Starts and Implications for Secondary Organic
617 Aerosol Formation, Environ Sci Technol, 53, 1706-1714, 10.1021/acs.est.8b05600,
618 2019.
- 619 Erickson, M. H., Gueneron, M., and Jobson, B. T.: Measuring long chain alkanes in
620 diesel engine exhaust by thermal desorption PTR-MS, Atmospheric Measurement
621 Techniques, 7, 225-239, 10.5194/amt-7-225-2014, 2014.
- 622 Gentner, D. R., Isaacman, G., Worton, D. R., Chan, A. W., Dallmann, T. R., Davis, L.,
623 Liu, S., Day, D. A., Russell, L. M., Wilson, K. R., Weber, R., Guha, A., Harley, R. A.,
624 and Goldstein, A. H.: Elucidating secondary organic aerosol from diesel and gasoline
625 vehicles through detailed characterization of organic carbon emissions, Proc Natl Acad
626 Sci U S A, 109, 18318-18323, 10.1073/pnas.1212272109, 2012.

627 Gentner, D. R., Worton, D. R., Isaacman, G., Davis, L. C., Dallmann, T. R., Wood, E.
628 C., Herndon, S. C., Goldstein, A. H., and Harley, R. A.: Chemical Composition of Gas-
629 Phase Organic Carbon Emissions from Motor Vehicles and Implications for Ozone
630 Production, *Environmental Science & Technology*, 47, 11837-11848,
631 10.1021/es401470e, 2013.

632 Gentner, D. R., Jathar, S. H., Gordon, T. D., Bahreini, R., Day, D. A., El Haddad, I.,
633 Hayes, P. L., Pieber, S. M., Platt, S. M., de Gouw, J., Goldstein, A. H., Harley, R. A.,
634 Jimenez, J. L., Prevot, A. S., and Robinson, A. L.: Review of Urban Secondary Organic
635 Aerosol Formation from Gasoline and Diesel Motor Vehicle Emissions, *Environ Sci*
636 *Technol*, 51, 1074-1093, 10.1021/acs.est.6b04509, 2017.

637 George, I. J., Hays, M. D., Herrington, J. S., Preston, W., Snow, R., Faircloth, J., George,
638 B. J., Long, T., and Baldauf, R. W.: Effects of Cold Temperature and Ethanol Content
639 on VOC Emissions from Light-Duty Gasoline Vehicles, *Environ Sci Technol*, 49,
640 13067-13074, 10.1021/acs.est.5b04102, 2015.

641 Guo, H., Zou, S. C., Tsai, W. Y., Chan, L. Y., and Blake, D. R.: Emission characteristics
642 of nonmethane hydrocarbons from private cars and taxis at different driving speeds in
643 Hong Kong, *Atmospheric Environment*, 45, 2711-2721,
644 10.1016/j.atmosenv.2011.02.053, 2011.

645 Han, C., Liu, R., Luo, H., Li, G., Ma, S., Chen, J., and An, T.: Pollution profiles of
646 volatile organic compounds from different urban functional areas in Guangzhou China
647 based on GC/MS and PTR-TOF-MS: Atmospheric environmental implications,
648 *Atmospheric Environment*, 214, 10.1016/j.atmosenv.2019.116843, 2019.

649 He, X., Yuan, B., Wu, C., Wang, S., Wang, C., Huangfu, Y., Qi, J., Ma, N., Xu, W.,
650 Wang, M., Chen, W., Su, H., Cheng, Y., and Shao, M.: Volatile organic compounds in
651 wintertime North China Plain: Insights from measurements of proton transfer reaction
652 time-of-flight mass spectrometer (PTR-ToF-MS), *Journal of Environmental Sciences*,
653 10.1016/j.jes.2021.08.010, 2022.

654 Huang, J., Yuan, Z., Duan, Y., Liu, D., Fu, Q., Liang, G., Li, F., and Huang, X.:
655 Quantification of temperature dependence of vehicle evaporative volatile organic
656 compound emissions from different fuel types in China, *Sci Total Environ*, 813, 152661,
657 10.1016/j.scitotenv.2021.152661, 2021.

658 http://e.jmrb.com/m/2008/11/17/10/m_182226.shtml, Access on 2009-12-10, 2008.

659 Kansal, A.: Sources and reactivity of NMHCs and VOCs in the atmosphere: a review,
660 *J Hazard Mater*, 166, 17-26, 10.1016/j.jhazmat.2008.11.048, 2009.

661 Koss, A. R., Sekimoto, K., Gilman, J. B., Selimovic, V., Coggon, M. M., Zarzana, K.
662 J., Yuan, B., Lerner, B. M., Brown, S. S., Jimenez, J. L., Krechmer, J., Roberts, J. M.,
663 Warneke, C., Yokelson, R. J., and de Gouw, J.: Non-methane organic gas emissions
664 from biomass burning: identification, quantification, and emission factors from PTR-
665 ToF during the FIREX 2016 laboratory experiment, *Atmospheric Chemistry and*
666 *Physics*, 18, 3299-3319, 10.5194/acp-18-3299-2018, 2018.

667 Kroll, J. H., Donahue, N. M., Jimenez, J. L., Kessler, S. H., Canagaratna, M. R., Wilson,
668 K. R., Altieri, K. E., Mazzoleni, L. R., Wozniak, A. S., Bluhm, H., Mysak, E. R., Smith,
669 J. D., Kolb, C. E., and Worsnop, D. R.: Carbon oxidation state as a metric for describing

670 the chemistry of atmospheric organic aerosol, *Nat Chem*, 3, 133-139,
671 10.1038/nchem.948, 2011.

672 Kumar, A., Sinha, V., Shabin, M., Hakkim, H., Bonsang, B., and Gros, V.: Non-methane
673 hydrocarbon (NMHC) fingerprints of major urban and agricultural emission sources for
674 use in source apportionment studies, *Atmospheric Chemistry and Physics*, 20, 12133-
675 12152, 10.5194/acp-20-12133-2020, 2020.

676 Laurikko, J.: Ambient temperature effect on automotive exhaust emissions: FTP and
677 ECE test cycle responses, *The Science of Environment*, 169, 195-204, 1995.

678 Li, B., Ho, S. S. H., Xue, Y., Huang, Y., Wang, L., Cheng, Y., Dai, W., Zhong, H., Cao,
679 J., and Lee, S.: Characterizations of volatile organic compounds (VOCs) from vehicular
680 emissions at roadside environment: The first comprehensive study in Northwestern
681 China, *Atmospheric Environment*, 161, 1-12, 10.1016/j.atmosenv.2017.04.029, 2017.

682 Li, T., Wang, Z., Yuan, B., Ye, C., Lin, Y., Wang, S., Sha, Q. e., Yuan, Z., Zheng, J., and
683 Shao, M.: Emissions of carboxylic acids, hydrogen cyanide (HCN) and isocyanic acid
684 (HNCO) from vehicle exhaust, *Atmospheric Environment*,
685 10.1016/j.atmosenv.2021.118218, 2021.

686 Li, X., Wu, Y., Yao, X., Zhang, S., Zhou, Y., and Fu, L.: Evaluation of the environmental
687 benefits of the enhanced vehicle inspection /maintenance program based on the short
688 transient loaded mode in Guangzhou (in Chinese), *Acta Scientiae Circumstantiae*, 32(1),
689 101-108, 10.13671/j.hjkxxb.2012.01.009, 2012.

690 Liao, S., Zhang, J., Yu, F., Zhu, M., Liu, J., Ou, J., Dong, H., Sha, Q., Zhong, Z., Xie,
691 Y., Luo, H., Zhang, L., and Zheng, J.: High Gaseous Nitrous Acid (HONO) Emissions
692 from Light-Duty Diesel Vehicles, *Environ Sci Technol*, 55, 200-208,
693 10.1021/acs.est.0c05599, 2021.

694 Liu, H., Man, H., Cui, H., Wang, Y., Deng, F., Wang, Y., Yang, X., Xiao, Q., Zhang, Q.,
695 Ding, Y., and He, K.: An updated emission inventory of vehicular VOCs and IVOCs in
696 China, *Atmospheric Chemistry and Physics*, 17, 12709-12724, 10.5194/acp-17-12709-
697 2017, 2017.

698 Liu, Y., Shao, M., Fu, L., Lu, S., Zeng, L., and Tang, D.: Source profiles of volatile
699 organic compounds (VOCs) measured in China: Part I, *Atmospheric Environment*, 42,
700 6247-6260, 10.1016/j.atmosenv.2008.01.070, 2008.

701 Liu, Y., Li, Y., Yuan, Z., Wang, H., Sha, Q., Lou, S., Liu, Y., Hao, Y., Duan, L., Ye, P.,
702 Zheng, J., Yuan, B., and Shao, M.: Identification of two main origins of intermediate-
703 volatility organic compound emissions from vehicles in China through two-phase
704 simultaneous characterization, *Environ Pollut*, 281, 117020,
705 10.1016/j.envpol.2021.117020, 2021.

706 Lu, Q., Zhao, Y., and Robinson, A. L.: Comprehensive organic emission profiles for
707 gasoline, diesel, and gas-turbine engines including intermediate and semi-volatile
708 organic compound emissions, *Atmospheric Chemistry and Physics*, 18, 17637-17654,
709 10.5194/acp-18-17637-2018, 2018.

710 Ly, B. T., Kajii, Y., Nguyen, T. Y., Shoji, K., Van, D. A., Do, T. N., Nghiem, T. D., and
711 Sakamoto, Y.: Characteristics of roadside volatile organic compounds in an urban area
712 dominated by gasoline vehicles, a case study in Hanoi, *Chemosphere*, 254, 126749,
713 10.1016/j.chemosphere.2020.126749, 2020.

714 Lyu, M., Bao, X., Zhu, R., and Matthews, R.: State-of-the-art outlook for light-duty
715 vehicle emission control standards and technologies in China, *Clean Technologies and*
716 *Environmental Policy*, 22, 757-771, 10.1007/s10098-020-01834-x, 2020.

717 May, A. A., Nguyen, N. T., Presto, A. A., Gordon, T. D., Lipsky, E. M., Karve, M.,
718 Gutierrez, A., Robertson, W. H., Zhang, M., Brandow, C., Chang, O., Chen, S., Cicero-
719 Fernandez, P., Dinkins, L., Fuentes, M., Huang, S.-M., Ling, R., Long, J., Maddox, C.,
720 Masetti, J., McCauley, E., Miguel, A., Na, K., Ong, R., Pang, Y., Rieger, P., Sax, T.,
721 Truong, T., Vo, T., Chattopadhyay, S., Maldonado, H., Maricq, M. M., and Robinson,
722 A. L.: Gas- and particle-phase primary emissions from in-use, on-road gasoline and
723 diesel vehicles, *Atmospheric Environment*, 88, 247-260,
724 10.1016/j.atmosenv.2014.01.046, 2014.

725 China Mobile Source Environmental Management Annual Report:
726 <http://www.mee.gov.cn/hjzl/sthjzk/ydyhjgl/201909/P020190905586230826402.pdf>,
727 2019.

728 Mo, Z., Shao, M., and Lu, S.: Compilation of a source profile database for hydrocarbon
729 and OVOC emissions in China, *Atmospheric Environment*, 143, 209-217,
730 10.1016/j.atmosenv.2016.08.025, 2016.

731 Ou, J., Zheng, J., Li, R., Huang, X., Zhong, Z., Zhong, L., and Lin, H.: Speciated OVOC
732 and VOC emission inventories and their implications for reactivity-based ozone control
733 strategy in the Pearl River Delta region, China, *Sci Total Environ*, 530-531, 393-402,
734 10.1016/j.scitotenv.2015.05.062, 2015.

735 Pang, X., Mu, Y., Yuan, J., and He, H.: Carbonyls emission from ethanol-blended
736 gasoline and biodiesel-ethanol-diesel used in engines, *Atmospheric Environment*, 42,
737 1349-1358, 10.1016/j.atmosenv.2007.10.075, 2008.

738 Parrish, D. D., Kuster, W. C., Shao, M., Yokouchi, Y., Kondo, Y., Goldan, P. D., de
739 Gouw, J. A., Koike, M., and Shirai, T.: Comparison of air pollutant emissions among
740 mega-cities, *Atmospheric Environment*, 43, 6435-6441,
741 10.1016/j.atmosenv.2009.06.024, 2009.

742 Qi, L., Liu, H., Shen, X., Fu, M., Huang, F., Man, H., Deng, F., Shaikh, A. A., Wang,
743 X., Dong, R., Song, C., and He, K.: Intermediate-Volatility Organic Compound
744 Emissions from Nonroad Construction Machinery under Different Operation Modes,
745 *Environ Sci Technol*, 53, 13832-13840, 10.1021/acs.est.9b01316, 2019.

746 Qiao, Y. Z., Wang, H. L., Huang, C., Chen, C. H., and Huang, H. Y.: Source profile and
747 chemical reactivity of volatile organic compounds from vehicle exhaust(in chinese),
748 *Environmental Science*, 33, 1071-1079, 2012.

749 Roy, A., Sonntag, D., Cook, R., Yanca, C., Schenk, C., and Choi, Y.: Effect of Ambient
750 Temperature on Total Organic Gas Speciation Profiles from Light-Duty Gasoline
751 Vehicle Exhaust, *Environmental Science & Technology*, 50, 6565-6573,
752 10.1021/acs.est.6b01081, 2016.

753 Rubin, J. I., Kean, A. J., Harley, R. A., Millet, D. B., and Goldstein, A. H.: Temperature
754 dependence of volatile organic compound evaporative emissions from motor vehicles,
755 *Journal of Geophysical Research: Atmospheres*, 111,
756 <https://doi.org/10.1029/2005JD006458>, 2006.

757 Schauer, J. J., Kleeman, M. J., Cass, G. R., and Simoneit, B. R., T.: Measurement of
758 Emissions from Air Pollution Sources. 2. C₁ through C₃₀ Organic Compounds from
759 Medium Duty Diesel Trucks, *Environmental Science & Technology*, 33, 1578-1587,
760 1999.

761 Seinfeld, J. H., and Pandis, S. N.: *Atmospheric chemistry and physics: from air
762 pollution to climate change*, John Wiley & Sons, Inc., Hoboken, 2006.

763 Sekimoto, K., Li, S.-M., Yuan, B., Koss, A., Coggon, M., Warneke, C., and de Gouw,
764 J.: Calculation of the sensitivity of proton-transfer-reaction mass spectrometry (PTR-
765 MS) for organic trace gases using molecular properties, *International Journal of Mass
766 Spectrometry*, 421, 71-94, 10.1016/j.ijms.2017.04.006, 2017.

767 Sha, Q., Zhu, M., Huang, H., Wang, Y., Huang, Z., Zhang, X., Tang, M., Lu, M., Chen,
768 C., Shi, B., Chen, Z., Wu, L., Zhong, Z., Li, C., Xu, Y., Yu, F., Jia, G., Liao, S., Cui, X.,
769 Liu, J., and Zheng, J.: A newly integrated dataset of volatile organic compounds (VOCs)
770 source profiles and implications for the future development of VOCs profiles in China,
771 *Sci Total Environ*, 793, 148348, 10.1016/j.scitotenv.2021.148348, 2021.

772 Shao, M., Zhang, Y., Zeng, L., Tang, X., Zhang, J., Zhong, L., and Wang, B.: Ground-
773 level ozone in the Pearl River Delta and the roles of VOC and NO_x in its production,
774 *Journal of Environmental Management*, 90, 512-518, 10.1016/j.jenvman.2007.12.008,
775 2009.

776 Shen, X., Lv, T., Zhang, X., Cao, X., Li, X., Wu, B., Yao, X., Shi, Y., Zhou, Q., Chen,
777 X., and Yao, Z.: Real-world emission characteristics of black carbon emitted by on-road
778 China IV and China V diesel trucks, *Science of The Total Environment*, 799, 149435,
779 <https://doi.org/10.1016/j.scitotenv.2021.149435>, 2021.

780 Song, C., Liu, Y., Sun, L., Zhang, Q., and Mao, H.: Emissions of volatile organic
781 compounds (VOCs) from gasoline- and liquified natural gas (LNG)-fueled vehicles in
782 tunnel studies, *Atmospheric Environment*, 234, 10.1016/j.atmosenv.2020.117626, 2020.

783 Stark, H., Yatavelli, R. L. N., Thompson, S. L., Kimmel, J. R., Cubison, M. J., Chhabra,
784 P. S., Canagaratna, M. R., Jayne, J. T., Worsnop, D. R., and Jimenez, J. L.: Methods to
785 extract molecular and bulk chemical information from series of complex mass spectra
786 with limited mass resolution, *International Journal of Mass Spectrometry*, 389, 26-38,
787 10.1016/j.ijms.2015.08.011, 2015.

788 Sulzer, P., Hartungen, E., Hanel, G., Feil, S., Winkler, K., Mutschlechner, P., Haidacher,
789 S., Schotchkowsky, R., Gunsch, D., Seehauser, H., Striednig, M., Jürschik, S., Breiev, K.,
790 Lanza, M., Herbig, J., Märk, L., Märk, T. D., and Jordan, A.: A Proton Transfer
791 Reaction-Quadrupole interface Time-Of-Flight Mass Spectrometer (PTR-QiTOF):
792 High speed due to extreme sensitivity, *International Journal of Mass Spectrometry*, 368,
793 1-5, 10.1016/j.ijms.2014.05.004, 2014.

794 Sun, W., Shao, M., Granier, C., Liu, Y., Ye, C. S., and Zheng, J. Y.: Long-Term Trends
795 of Anthropogenic SO₂, NO_x, CO, and NMVOCs Emissions in China, *Earth's Future*, 6,
796 1112-1133, 10.1029/2018ef000822, 2018.

797 Tsai, J.-H., Chang, S.-Y., and Chiang, H.-L.: Volatile organic compounds from the
798 exhaust of light-duty diesel vehicles, *Atmospheric Environment*, 61, 499-506,
799 10.1016/j.atmosenv.2012.07.078, 2012.

800 Wallington, T. J., Lambert, C. K., and Ruona, W. C.: Diesel vehicles and sustainable
801 mobility in the U.S, *Energy Policy*, 54, 47-53, 10.1016/j.enpol.2011.11.068, 2013.

802 Wang, C., Yuan, B., Wu, C., Wang, S., Qi, J., Wang, B., Wang, Z., Hu, W., Chen, W.,
803 Ye, C., Wang, W., Sun, Y., Wang, C., Huang, S., Song, W., Wang, X., Yang, S., Zhang,
804 S., Xu, W., Ma, N., Zhang, Z., Jiang, B., Su, H., Cheng, Y., Wang, X., and Shao, M.:
805 Measurements of higher alkanes using NO^+ chemical ionization in PTR-ToF-MS:
806 important contributions of higher alkanes to secondary organic aerosols in China,
807 *Atmospheric Chemistry and Physics*, 20, 14123-14138, 10.5194/acp-20-14123-2020,
808 2020a.

809 Wang, H., L. , Jing, S., A. , Lou, S., R. , Hu, Q., Y. , Li, L., Tao, S., K. , Huang, C., Qiao,
810 L., P. , and Chen, C., H.: Volatile organic compounds (VOCs) source profiles of on-
811 road vehicle emissions in China, *Sci Total Environ*, 607-608, 253-261,
812 10.1016/j.scitotenv.2017.07.001, 2017.

813 Wang, J., Jin, L., Gao, J., Shi, J., Zhao, Y., Liu, S., Jin, T., Bai, Z., and Wu, C. Y.:
814 Investigation of speciated VOC in gasoline vehicular exhaust under ECE and EUDC
815 test cycles, *Sci Total Environ*, 445-446, 110-116, 10.1016/j.scitotenv.2012.12.044, 2013.

816 Wang, M., Li, S., Zhu, R., Zhang, R., Zu, L., Wang, Y., and Bao, X.: On-road tailpipe
817 emission characteristics and ozone formation potentials of VOCs from gasoline, diesel
818 and liquefied petroleum gas fueled vehicles, *Atmospheric Environment*,
819 10.1016/j.atmosenv.2020.117294, 2020b.

820 Wang, Z., Yuan, B., Ye, C., Roberts, J., Wisthaler, A., Lin, Y., Li, T., Wu, C., Peng, Y.,
821 Wang, C., Wang, S., Yang, S., Wang, B., Qi, J., Wang, C., Song, W., Hu, W., Wang, X.,
822 Xu, W., Ma, N., Kuang, Y., Tao, J., Zhang, Z., Su, H., Cheng, Y., Wang, X., and Shao,
823 M.: High Concentrations of Atmospheric Isocyanic Acid (HNCO) Produced from
824 Secondary Sources in China, *Environmental Science & Technology*,
825 10.1021/acs.est.0c02843, 2020c.

826 Wu, C., Wang, C., Wang, S., Wang, W., Yuan, B., Qi, J., Wang, B., Wang, H., Wang, C.,
827 Song, W., Wang, X., Hu, W., Lou, S., Ye, C., Peng, Y., Wang, Z., Huangfu, Y., Xie, Y.,
828 Zhu, M., Zheng, J., Wang, X., Jiang, B., Zhang, Z., and Shao, M.: Measurement report:
829 Important contributions of oxygenated compounds to emissions and chemistry of
830 volatile organic compounds in urban air, *Atmospheric Chemistry and Physics*, 20,
831 14769-14785, 10.5194/acp-20-14769-2020, 2020.

832 Wu, R., Bo, Y., Li, J., Li, L., Li, Y., and Xie, S.: Method to establish the emission
833 inventory of anthropogenic volatile organic compounds in China and its application in
834 the period 2008–2012, *Atmospheric Environment*, 127, 244-254,
835 10.1016/j.atmosenv.2015.12.015, 2016.

836 Wu, Y., Zhang, S., Hao, J., Liu, H., Wu, X., Hu, J., Walsh, M. P., Wallington, T. J.,
837 Zhang, K. M., and Stevanovic, S.: On-road vehicle emissions and their control in China:
838 A review and outlook, *Sci Total Environ*, 574, 332-349,
839 10.1016/j.scitotenv.2016.09.040, 2017.

840 Yang, W., Zhang, Q., Wang, J., Zhou, C., Zhang, Y., and Pan, Z.: Emission
841 characteristics and ozone formation potentials of VOCs from gasoline passenger cars
842 at different driving modes, *Atmospheric Pollution Research*, 9, 804-813,
843 10.1016/j.apr.2018.01.002, 2018.

844 Yao, S., Liu, Z., and Qi, Z.: Test System for Exhaust Pollutants from Light-duty
845 Gasoline Vehicle under Short Transient Driving Cycle (in Chinese), Shanghai
846 Environmental Sciences, 10, 722-728, 2003.

847 Yao, Z., Shen, X., Ye, Y., Cao, X., Jiang, X., Zhang, Y., and He, K.: On-road emission
848 characteristics of VOCs from diesel trucks in Beijing, China, Atmospheric Environment,
849 103, 87-93, 10.1016/j.atmosenv.2014.12.028, 2015.

850 Ye, C., Yuan, B., Lin, Y., Wang, Z., Hu, W., Li, T., Chen, W., Wu, C., Wang, C., Huang,
851 S., Qi, J., Wang, B., Wang, C., Song, W., Wang, X., Zheng, E., Krechmer, J. E., Ye, P.,
852 Zhang, Z., Wang, X., Worsnop, D. R., and Shao, M.: Chemical characterization of
853 oxygenated organic compounds in the gas phase and particle phase using iodide CIMS
854 with FIGAERO in urban air, Atmospheric Chemistry and Physics, 21, 8455-8478,
855 10.5194/acp-21-8455-2021, 2021.

856 Yuan, B., Koss, A. R., Warneke, C., Coggon, M., Sekimoto, K., and de Gouw, J. A.:
857 Proton-Transfer-Reaction Mass Spectrometry: Applications in Atmospheric Sciences,
858 Chemical Reviews, 117, 13187-13229, 10.1021/acs.chemrev.7b00325, 2017.

859 Yue, X., Wu, Y., Hao, J., Pang, Y., Ma, Y., Li, Y., Li, B., and Bao, X.: Fuel quality
860 management versus vehicle emission control in China, status quo and future
861 perspectives, Energy Policy, 79, 87-98, <https://doi.org/10.1016/j.enpol.2015.01.009>,
862 2015.

863 Zavala, M., Herndon, S. C., Slott, R. S., Dunlea, E. J., Marr, L. C., Shorter, J. H.,
864 Zahniser, M., Knighton, W. B., Rogers, T. M., Kolb, C. E., Molina, L. T., and Molina,
865 M. J.: Characterization of on-road vehicle emissions in the Mexico City Metropolitan
866 Area using a mobile laboratory in chase and fleet average measurement modes during
867 the MCMA-2003 field campaign, Atmospheric Chemistry and Physics, 6, 5129-5142,
868 10.5194/acp-6-5129-2006, 2006.

869 Zavala, M., Herndon, S. C., Wood, E. C., Jayne, J. T., Nelson, D. D., Trimborn, A. M.,
870 Dunlea, E., Knighton, W. B., Mendoza, A., Allen, D. T., Kolb, C. E., Molina, M. J., and
871 Molina, L. T.: Comparison of emissions from on-road sources using a mobile laboratory
872 under various driving and operational sampling modes, Atmospheric Chemistry and
873 Physics, 9, 1-14, 10.5194/acp-9-1-2009, 2009.

874 Zhang, Q., Wu, L., Fang, X., Liu, M., Zhang, J., Shao, M., Lu, S., and Mao, H.:
875 Emission factors of volatile organic compounds (VOCs) based on the detailed vehicle
876 classification in a tunnel study, Sci Total Environ, 624, 878-886,
877 10.1016/j.scitotenv.2017.12.171, 2018.

878 Zhao, Y., Saleh, R., Saliba, G., Presto, A. A., Gordon, T. D., Drozd, G. T., Goldstein, A.
879 H., Donahue, N. M., and Robinson, A. L.: Reducing secondary organic aerosol
880 formation from gasoline vehicle exhaust, Proc Natl Acad Sci U S A, 114, 6984-6989,
881 10.1073/pnas.1620911114, 2017.

882 Zhou, H., Zhao, H., Hu, J., Li, M., Feng, Q., Qi, J., Shi, Z., Mao, H., and Jin, T.: Primary
883 particulate matter emissions and estimates of secondary organic aerosol formation
884 potential from the exhaust of a China V diesel engine, Atmospheric Environment, 218,
885 116987, <https://doi.org/10.1016/j.atmosenv.2019.116987>, 2019.

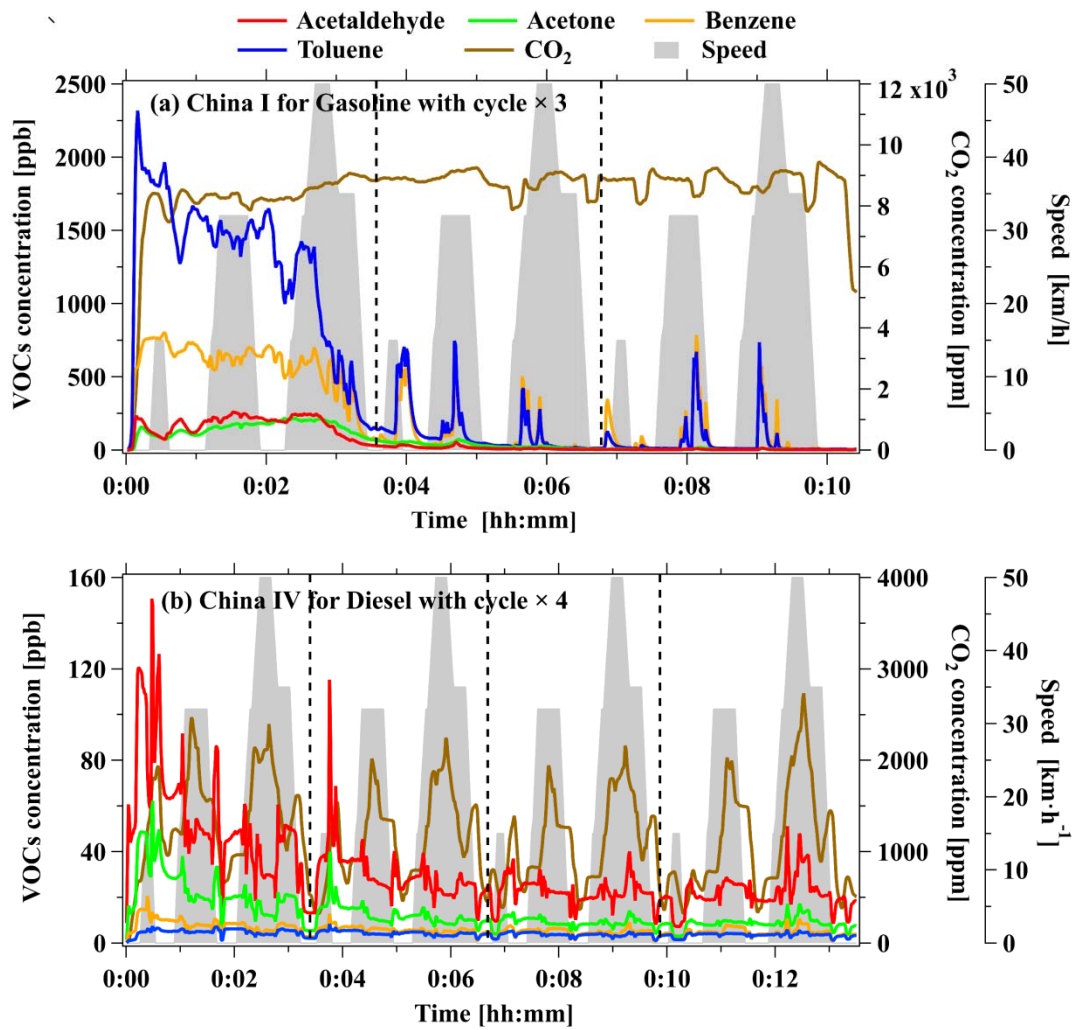
886 Zhu, M., Dong, H., Yu, F., Liao, S., Xie, Y., Liu, J., Sha, Q., Zhong, Z., Zeng, L., and
887 Zheng, J.: A New Portable Instrument for Online Measurements of Formaldehyde:

888 From Ambient to Mobile Emission Sources, *Environmental Science & Technology*
889 *Letters*, 7, 292-297, 10.1021/acs.estlett.0c00169, 2020.

890 Ziemann, P. J., and Atkinson, R.: Kinetics, products, and mechanisms of secondary
891 organic aerosol formation, *Chem Soc Rev*, 41, 6582-6605, 10.1039/c2cs35122f, 2012.

892

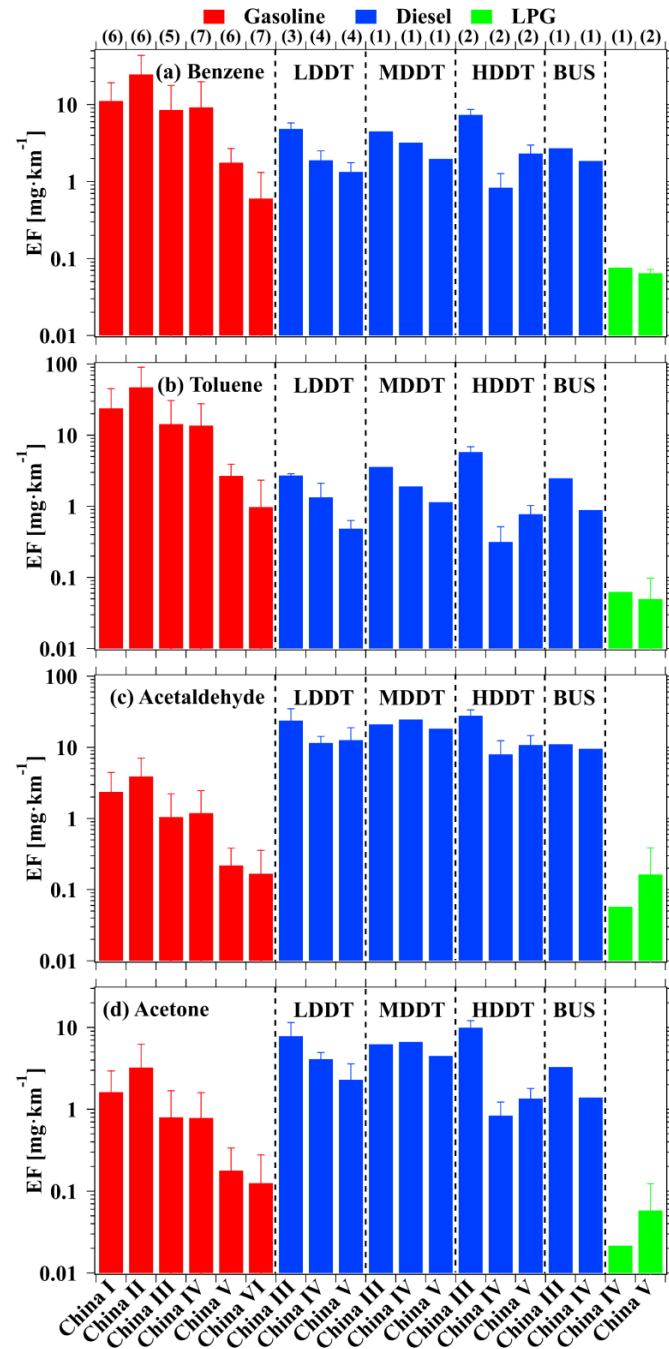
893



894

895 **Figure 1.** Real-time concentrations of acetaldehyde, acetone, benzene, toluene, and
 896 CO₂ for (a) a gasoline vehicle with emission standard of China I and (b) a light-duty
 897 diesel vehicle (LDDV) with emission standard of China IV. The two vehicles were both
 898 cold started. The gray shadows represent the speed of the vehicles on the chassis
 899 dynamometer.

900



901

902 **Figure 2.** The determined average mileage-based emission factors ($\text{mg}\cdot\text{km}^{-1}$) for (a)

903 benzene, (b) toluene, (c) acetaldehyde, and (d) acetone for vehicles with different

904 emission standards. The numbers above the top axis represent the number of all

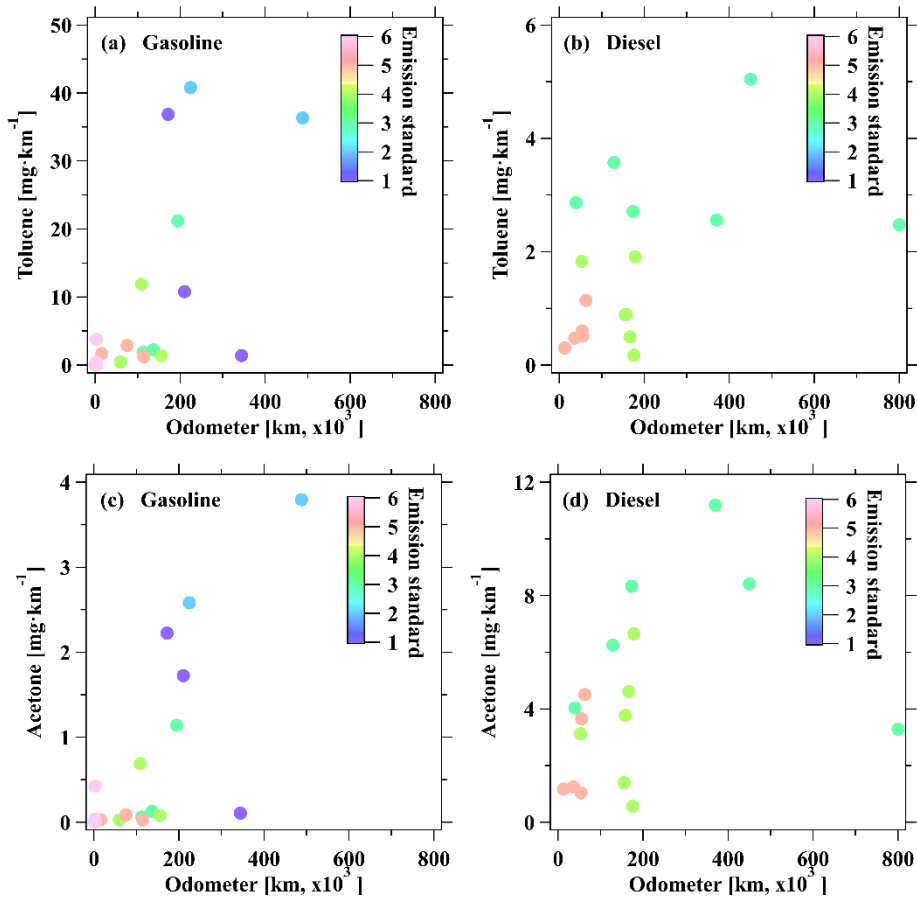
905 experiments (including multiple measurements for individual test vehicle) for each

906 emission standard. LDDT, MDDT, HDDT, and BUS represent light-duty-diesel-truck,

907 middle-duty-diesel-truck, heavy-duty-diesel-truck, and bus, respectively. Error bars

908 represent standard deviations of emission factors for the specific emission standard.

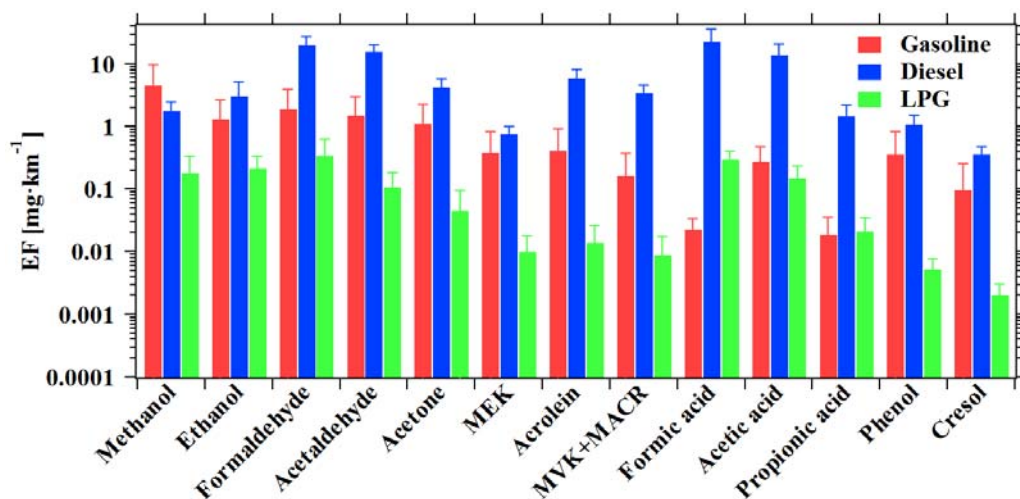
909



910

911 **Figure 3.** Scatterplot of the emission factor of toluene in (a) gasoline and (b) diesel
 912 vehicles, and acetone in (c) gasoline and (d) diesel vehicles during the hot start based
 913 on the odometer for each vehicle.

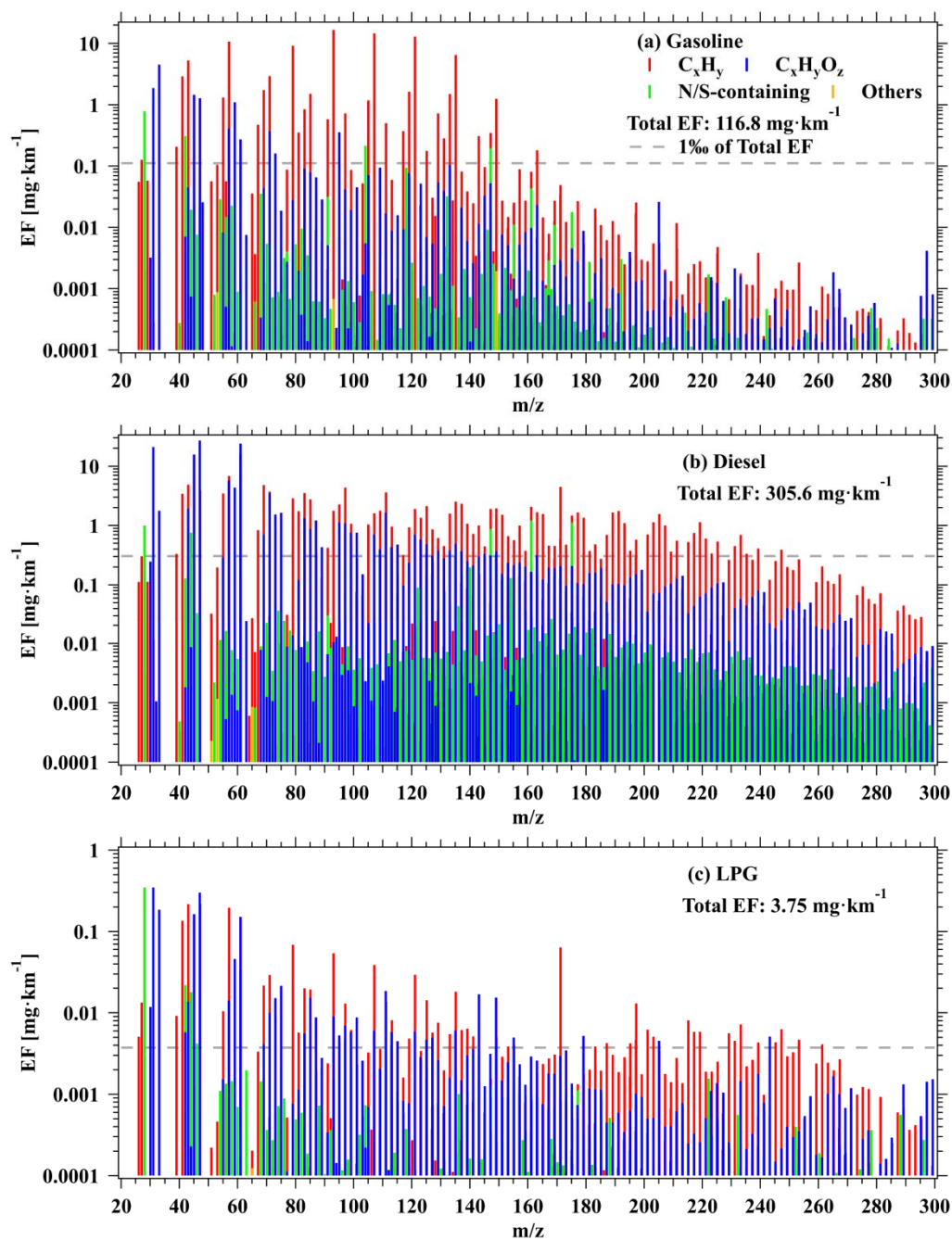
914



915

916 **Figure 4.** The determined emission factors of representative OVOC species from
 917 different types of vehicles. Error bars represent standard deviations of the emission
 918 factors for the VOCs.

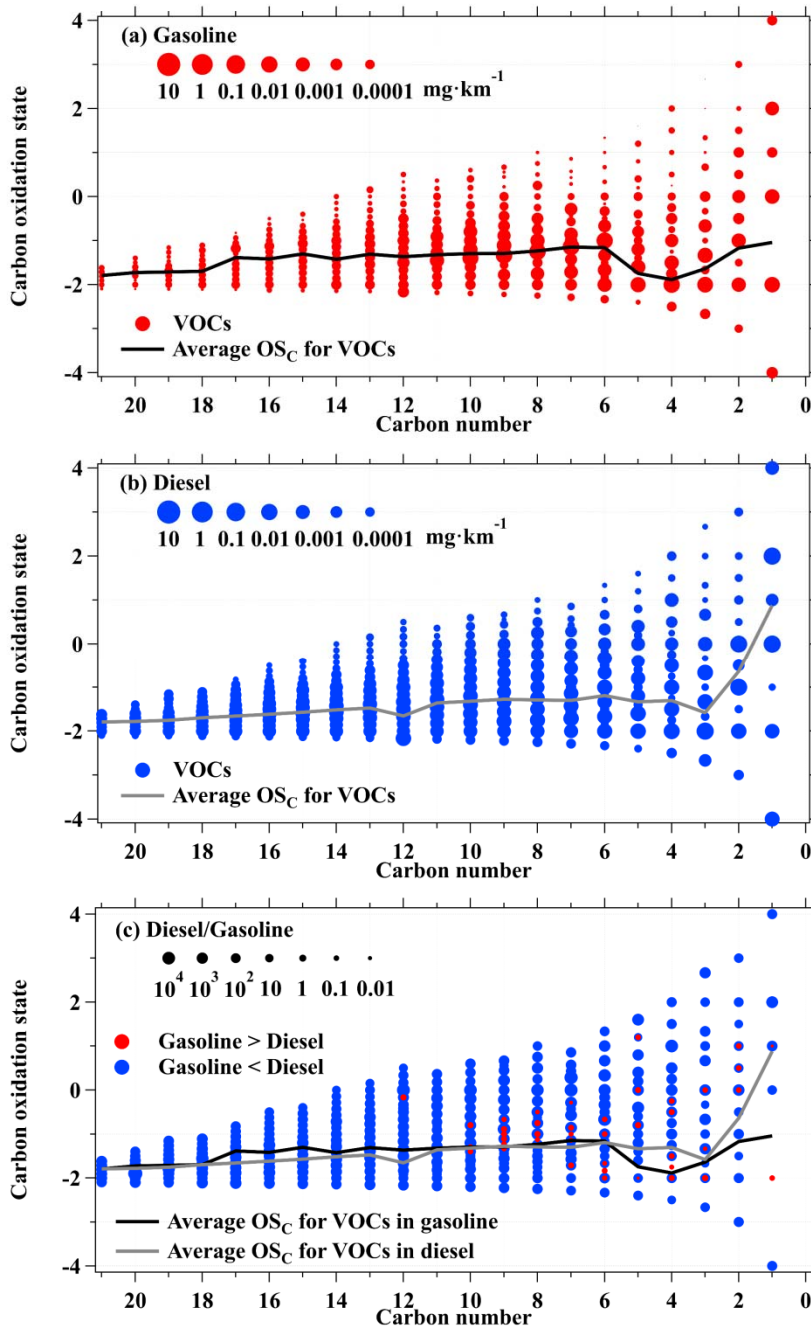
919



920

921 **Figure 5.** The determined average mileage-based emission factors of VOC species
 922 measured by PTR-ToF-MS from (a) gasoline, (b) diesel, and (c) LPG vehicles. The
 923 gray dashed lines represent 1% of total VOCs emission factors.

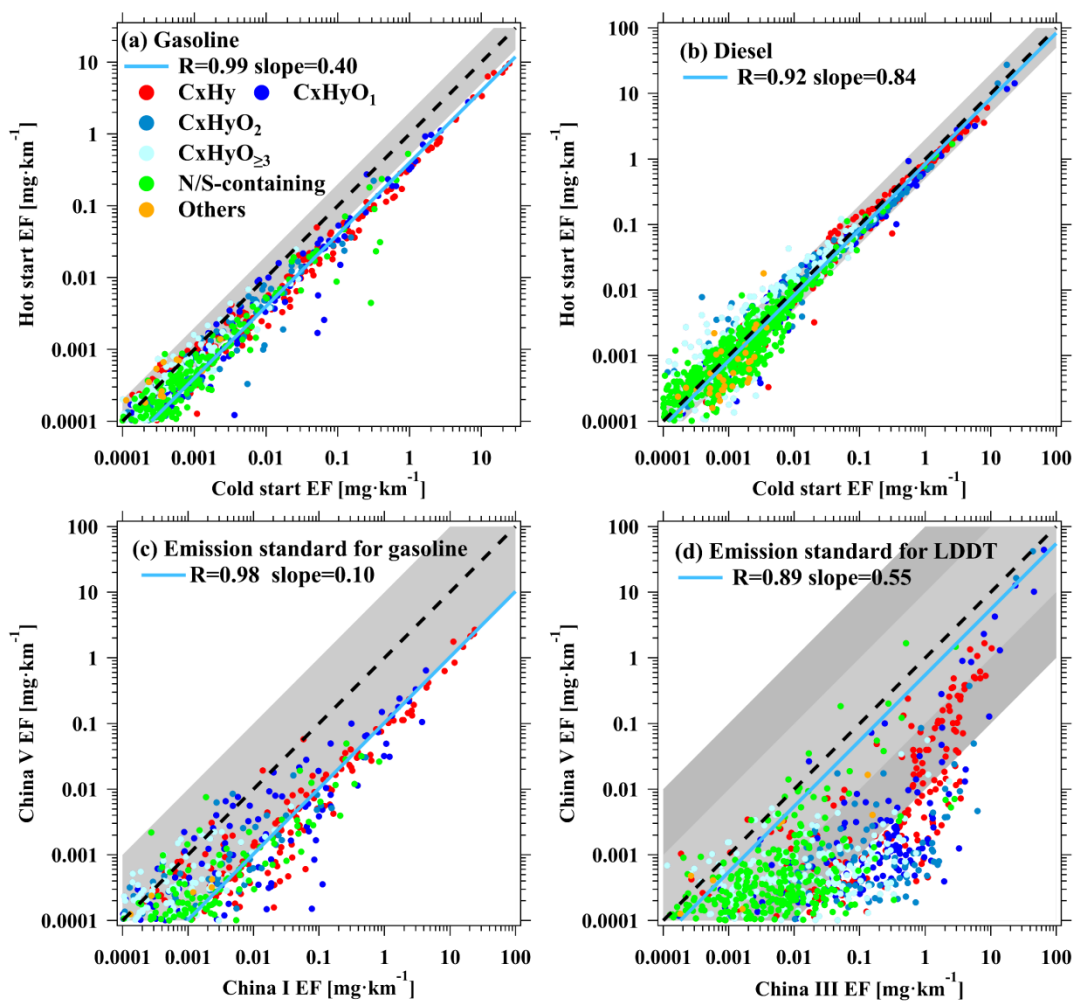
924



925

926 **Figure 6.** The two-dimensional space of $\overline{OS}_C - n_C$ with data points sized coded using
 927 emission factors of VOC species from (a) gasoline and (b) diesel vehicles, and (c) the
 928 ratio of emission factors of diesel vehicle relative to gasoline vehicle. The black and
 929 gray lines are the average \overline{OS}_C of each carbon number for VOC species in gasoline and
 930 diesel vehicles, respectively.

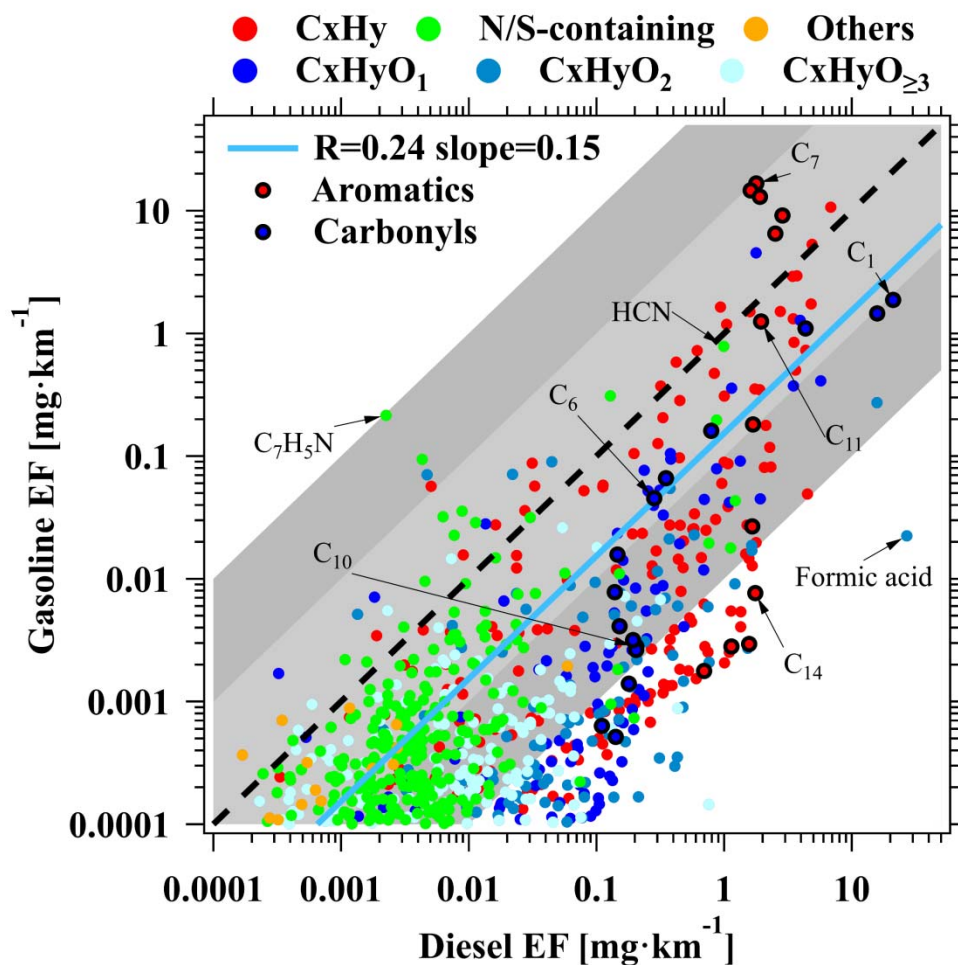
931



932

933 **Figure 7.** Scatterplots of VOCs emission factors between cold start and hot start for
 934 gasoline (a) and diesel vehicles (b). Scatterplots of VOCs emission factors between
 935 China I and China V emission standard for gasoline vehicles (c) and between China III
 936 and China V emission standard for diesel vehicles (d). Each data point indicates a VOC
 937 species measured by PTR-ToF-MS. The blue lines are the fitted results for all data
 938 points. The black dashed lines represent 1:1 ratio, and the shaded areas represent ratios
 939 of a factor of 2 in (a) and (b), and a factor of 10 and 100 in (c) and (d).

940



941

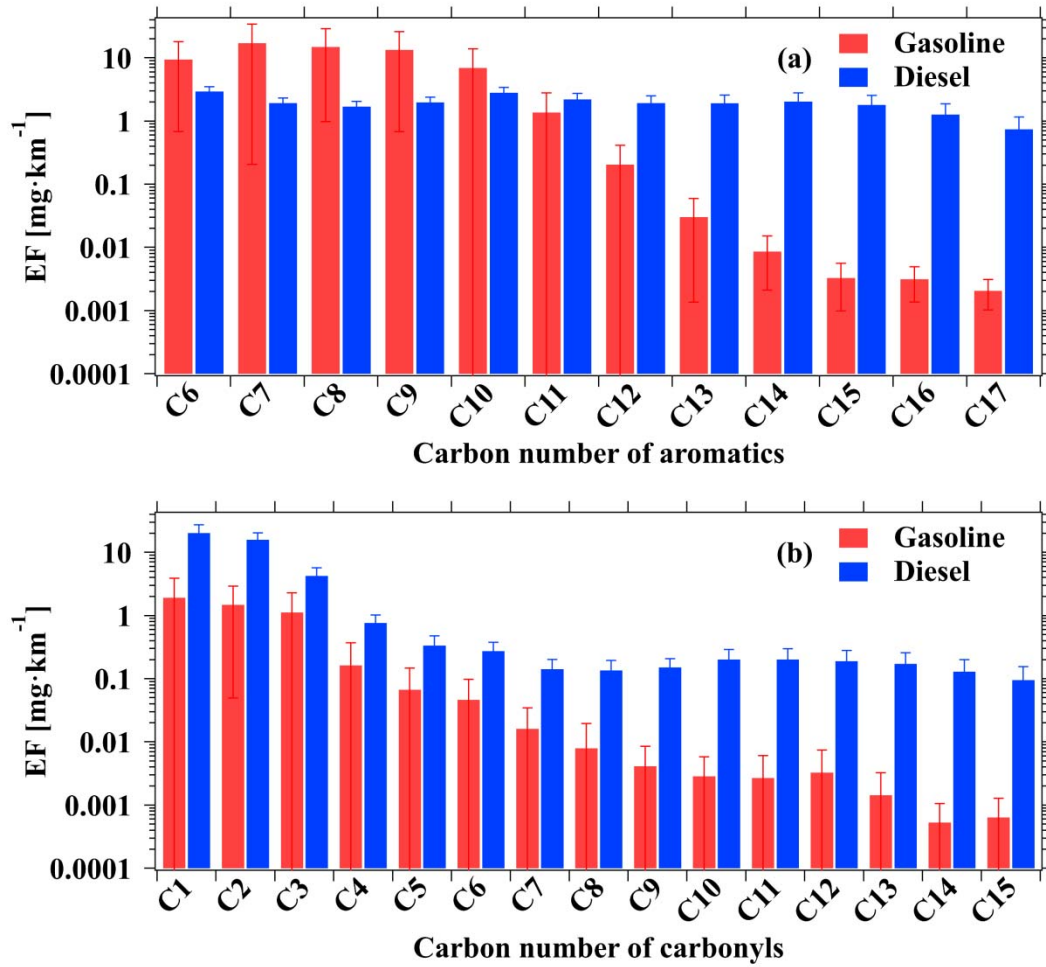
942 **Figure 8.** Scatterplot of VOCs emission factors between gasoline and diesel vehicles.

943 Each data point indicates a VOC species measured by PTR-ToF-MS. The blue line is

944 the fitted result for all data points. The black line represents 1:1 ratio, and the shaded

945 areas represent ratios of a factor of 10 and 100.

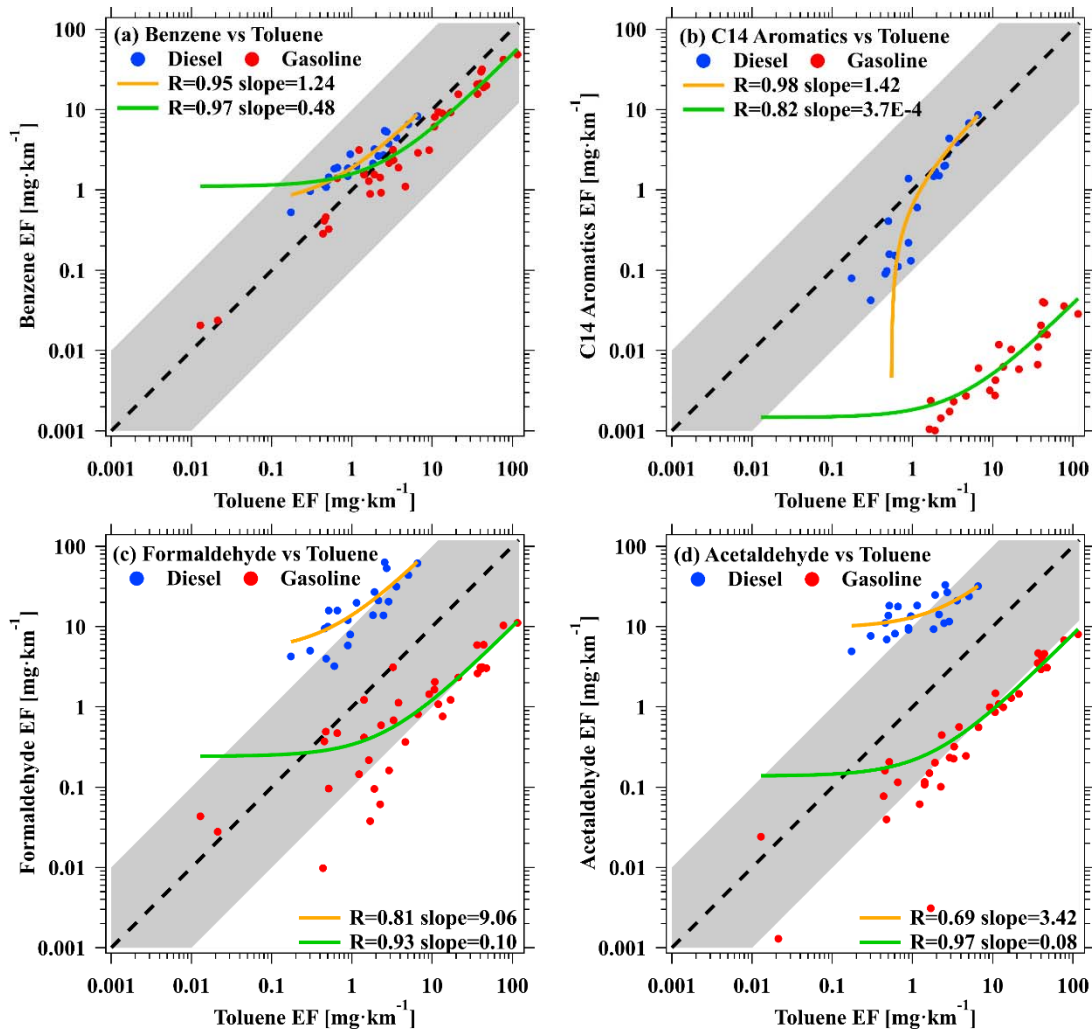
946



947

948 **Figure 9.** The determined emission factors of (a) aromatics and (b) carbonyls for each
 949 carbon number from gasoline and diesel vehicles. Error bars represent standard
 950 deviations of the emission factors for the VOCs of different carbon number.

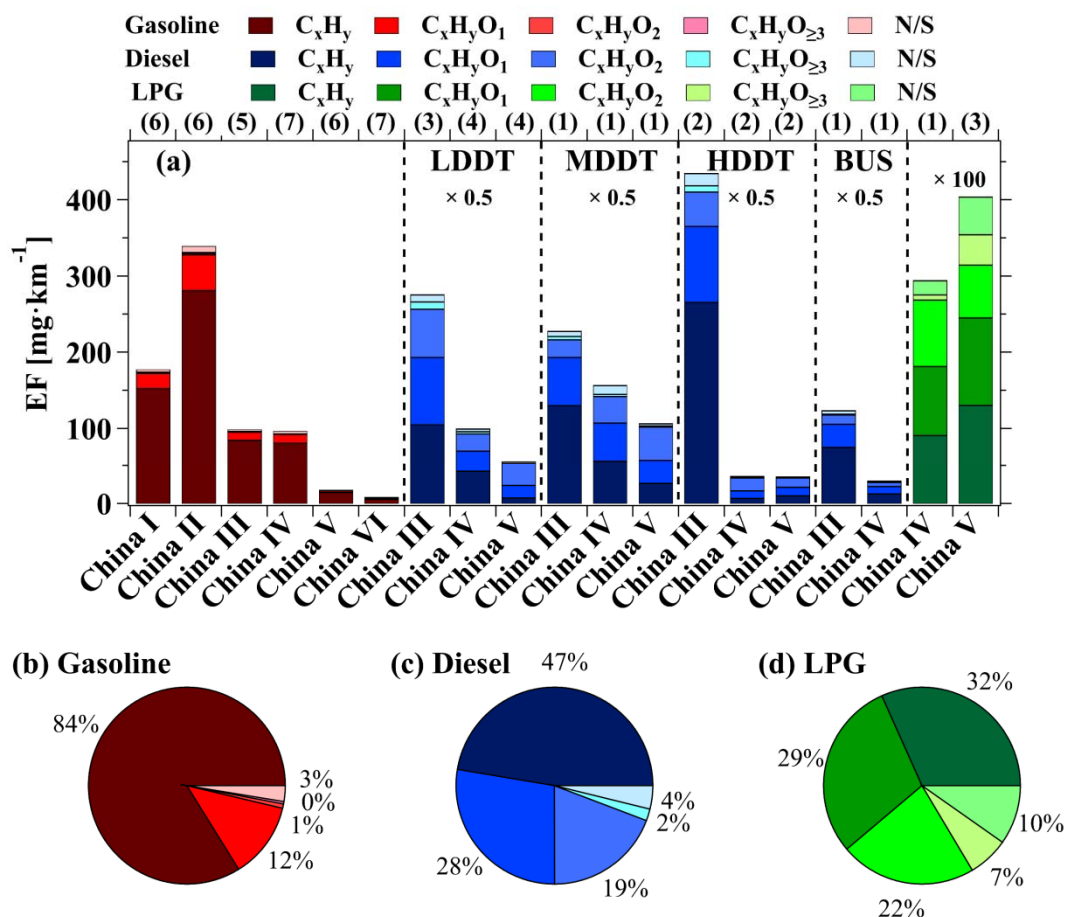
951



952

953 **Figure 10.** Scatterplots of the determined mileage-based emission factors of (a)
 954 benzene versus toluene, (b) C₁₄ aromatics versus toluene, (c) formaldehyde versus
 955 toluene, and (d) acetaldehyde versus toluene for gasoline and diesel vehicles. Each data
 956 point represents each test vehicle in this study. The green and orange lines are the fitted
 957 results for gasoline and diesel vehicle. The black line represents 1:1 ratio, and the
 958 shaded areas represent ratio of a factor of 10. The green and orange line are the fits to
 959 gasoline and diesel points in each plot. Note that these linear fits are shown in curves
 960 in log-log space as the result of non-zero y-intercept.

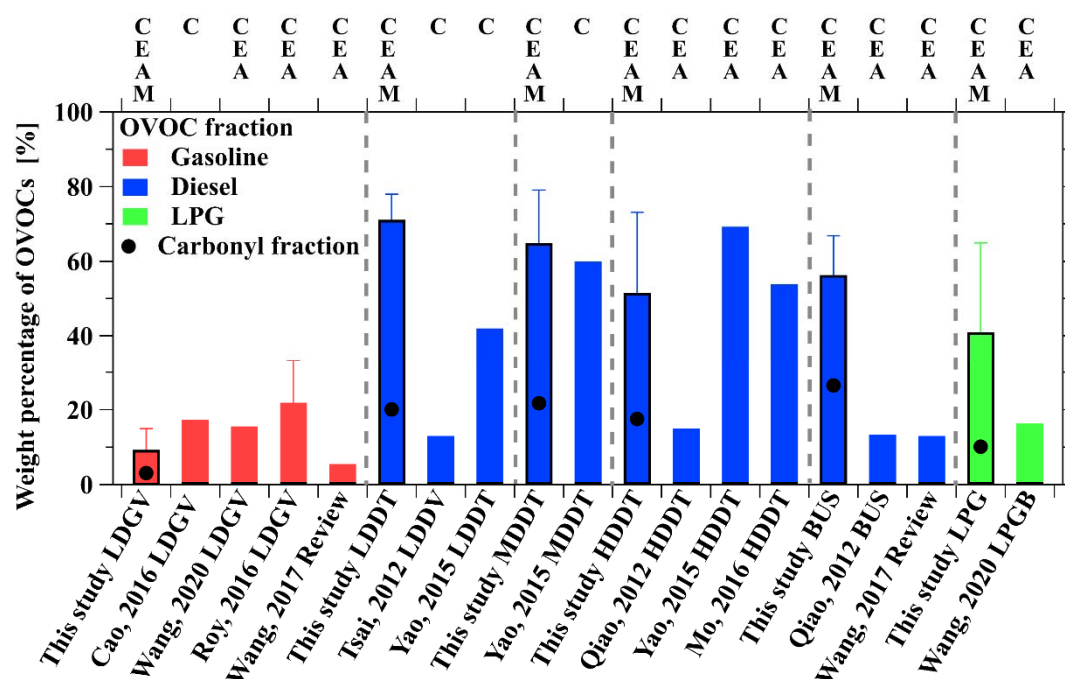
961



962

963 **Figure 11.** (a) The determined average emission factors for different emission standard
 964 from gasoline, diesel ($\times 0.5$), and LPG ($\times 100$) vehicles measured by PTR-ToF-MS. The
 965 different ion categories are discussed in the manuscript. Fractions of the determined
 966 average emission factors of VOCs ions in different ion categories from (b) gasoline, (c)
 967 diesel, and (d) LPG vehicles. The numbers above the top axis represent the number of
 968 all experiments (including multiple measurements for individual test vehicle) for each
 969 emission standard.

970



972

973 **Figure 12.** Comparison of OVOCs fractions determined in this study and those in
 974 previous studies. Error bars represent the standard deviations of the weight percentage
 975 of OVOCs. The C, E, A, M above the top axis represent the four groups of OVOCs
 976 measured in this study or previous studies, including Carbonyl: C, Ester/Ether: E,
 977 Alcohol: A, Multiple-functional: M.